Responses to the Interactive comments on "Simulating age of air and distribution of SF_6 in the stratosphere with SILAM model"

Rostislav Kouznetsov[1,2], Mikhail Sofiev[1], Julius Vira[1,3], and Gabriele Stiller[4]

[1]Finnish Meteorological Institute, Helsinki, Finland
[2]Obukhov Institute for Atmospheric Physics, Moscow, Russia
[3]Currently at Cornell University, Ithaca, NY, USA
[4]Karlsruhe Institute of Technology, Karlsruhe, Germany

Correspondence: Rostislav Kouznetsov (Rostislav.Kouznetsov@fmi.fi)

1 Response to the Interactive comment RC1

This study presents simulations of SF6, and determinations of age of air from this tracer, carried out with a chemical transport model (SILAM). It contains useful material that should be suitable for publication. However, it also includes lengthy discussions of molecular diffusion effects that do not appear to be relevant, while omitting essential information on other aspects of transport that are essential for understanding the distribution of SF6.

The model's upper boundary is at 65 km (0.1 hPa). At this altitude, the effects of molecular diffusion are essentially negligible compared to the strong vertical mixing generated by breaking gravity waves, and to advection by the mean meridional circulation forced by wave breaking. Thus, the discussion of molecular diffusion, and of simulations that prescribe unrealistically low values of diffusivity in the upper stratosphere and mesosphere are not very useful and should be omitted in a revised version.

On the other hand, there is little if any discussion of mean meridional advection and how the vertical flux due to the mean meridional circulation is handled in SILAM. The model uses dynamical fields from ERA-Interim, which presumably include the effects of whatever gravity wave parameterization is used in that reanalysis. Thus, vertical fluxes due to mean meridional advection should not be negligible near the upper boundary of SILAM, but the paper does not mention advective transport at all, or how mean advective fluxes are handled at the upper boundary.

Finally, the study does not emphasize enough the role of SF6 loss by the electron attachment mechanism, which becomes fast in the mesosphere (Fig, 1) and is essential for simulating the distribution of SF6, as the WACCM results shown in Fig. 6 (which do not include this loss mechanism) make clear.

I view of all of this, I do not believe the paper is suitable for publication as it stands, but could be made so if revised to (1) eliminate irrelevant material on molecular diffusion; (2) use realistic profiles of eddy diffusion that could be obtained from any high-top model that parameterizes gravity wave breaking; (3) explain explicitly how mean meridional advective fluxes are handled at the upper boundary of SILAM; (4) document how these fluxes affect the distribution of SF6; and (5) emphasize the

role of SF6 loss via electron attachment, which is evidently much more important than photolysis. Specific comments on these and other issues can be found below.

Response: Thank you very much for your valuable comments and nice and concise summary of the major points. Here are the responses for them.

(1) eliminate irrelevant material on molecular diffusion;

We would not agree that molecular diffusion is irrelevant. The range of magnitudes for turbulent diffusion mentioned below in the comment for line. 387 ($10^{-3} - 10^{2}\ \mathrm{m^2 s^{-1}}$) overlaps with the range of molecular diffusivities in the upper stratosphere and mesosphere ($10^{-3} - 10^{-1}\ \mathrm{m^2 s^{-1}}$, see Fig. 1 of the manuscript). Thus molecular diffusivity cannot be considered as negligible in general.

The study deals with turbulent diffusion. Molecular diffusion poses quite well defined lower limit for diffusive transport. Consideration of molecular diffusion helps to interpret results of parametrizations for turbulent diffusion as irrelevant when they fall below the molecular diffusion. In particular, without molecular diffusion it would be impossible to draw a conclusion that regardless the eddy diffusivity or advective transport the lifetime of SF6 in the upper model layer of our simulations is at most 60 days. This conclusion is at least interesting, to our view.

Moreover, to our best knowledge, the present study is the only one to date that explicitly quantifies the role of gravitational separation on the SF6 distribution in the atmosphere. The molecular diffusion is the mechanism responsible for gravitational separation.

Thus we decided to keep corresponding parts of the paper.

(2) use realistic profiles of eddy diffusion that could be obtained from any high-top model that parameterizes gravity wave breaking

We agree that some of the turbulent profiles tested in the paper look unrealistic - and that was the very reason for testing several options. As we saw in the literature and pointed out in the paper, there are several parameterizations and estimates of the turbulence in the upper troposphere and the stratosphere - and they do not agree with each other. Therefore, in the paper we evaluated the sensitivity of the AoA and SF6 to a variety of assumptions about the absolute levels of turbulent diffusion but preferred not to select the one out of many.

We agree that use of more sophisticated schemes could bring extra information but it would also require resolving the vertical and horizontal air motions near and above the model lid $0.1\,\mathrm{hPa}$ both in vertical and in horizontal dimensions, consistent matching these motions to the air-flux fields we derive from ERA-Interim winds, involvement of ERA5 with higher vertical coverage, etc. All these deserve a separate study and can hardly be fit into the current paper.

As we have specified in Introduction, the aim of the study is to provide consistent simulations simultaneously reproducing the spatio-temporal distribution of AoA and the $\mathrm{SF_6}$ mixing ratio in the troposphere and stratosphere.

The way the simulations were made resulted in a distributions of $\mathrm{SF_6}$ in troposphere and lower stratosphere that agree quite well to both balloon measurements and MIPAS retrievals.

(3) explain explicitly how mean meridional advective fluxes are handled at the upper boundary of SILAM;

We are grateful for pointing out this omission. The model uses a "hardtop" wind diagnostic procedure, forcing zero vertical wind at the domain top ($0.1\,\mathrm{hPa}$), thus precluding any advective fluxes through the lid. This is an immediate consequence of the topmost level of the ERA-Interim reanalysis at $0.1\,\mathrm{hPa}$.

Therefore, the hard-top assumption is the only that allows for the global air-mass conservation. The statement somehow slipped out of the "Simulation setup" section. Added now at the beginning of Sec. 3.

The diffusive fluxes through the domain top are however allowed.

(4) document how these fluxes affect the distribution of SF6

The ways the fluxes through the domain top affect distribution of SF_6 are analyzed in Section "Sensitivity and validation of SF6 simulations".

(5) emphasize the role of SF6 loss via electron attachment, which is evidently much more important than photolysis

We fully agree that electron attachment is much more important than photolysis, as it has been shown by Totterdill et al. (2015). A brief overview of relative role of electron attachment and photolysis is added to the "SF6 destruction" section.

Explicit mention of electron attachment as the mechanism for mesospheric loss is added to the Conclusions.

Specific comments (line number)

(72) "Silam": This is an undefined acronym. If you are going to use it here you need to define it here, not in the next section. Note also that you write "Silam" here and "SILAM" elsewhere. Please pick one form and stick with it throughout the text.

Response: The acronym has been explained, "Silam" has been changed to "SILAM" throughout the paper.

(129) "10 hPa": The conventional units of pressure in the atmospheric sciences are hPa (which are equivalent to the now deprecated mb). You might wish to consider changing references to pressure levels to units of hPa to avoid confusion (thus, 0.1 hPa in this instance).

Response: Pressure units were to hPa throughout the paper.

(131) "effect of diffusion of SF6 to the upper layers": Transport through the 0.1 hPa (10 Pa) surface is not solely (or at some latitudes even mainly) due to diffusion; mean meridional advection is important, especially in the polar regions.

Response: As we had a lid at 0.1hPa imposed by ERA-Interim, no regular mass fluxes are possible through the domain top in our simulations. The paragraph has been rephrased to avoid the word "diffusion" here. The role of a regular transport is discussed in the "Discussion section".

(167) "higher than . . . accepted in models": It is not clear what this means. What models are you referring to? Global models run at practical horizontal resolution do not produce large vertical diffusivity due to the explicitly resolved motions. However, all recent such models include parameterizations of (unresolved) mesoscale gravity wave breaking. Vertical diffusion coefficients, Kzz, can be estimated from these parameterizations, and they produce values of Kzz that vary strongly with altitude, latitude and season. Thus, a single, global Kzz profile is unlikely to capture accurately the role of vertical diffusion. See also comment at line 387.

Response: The expression has been replaced with a more precise reference to the ERA5 dataset. Applying these parameterizations in SILAM would be certainly interesting to do. However, these parameterizations tend to disagree with each other

and with (few) observations, which also implies additional research for the reasonable choice of a particular parametrization. In the current study we chose rather to evaluate the sensitivity to Kz levels than to attempt to find the best-fitting formulations. This topic has been included in our plans for the next studies that will be driven with ERA-5.

(168) "in order to cover the whole range of Kz": I think what you mean to say here is "to cover a range of vertical profiles of Kz". Is that so?

Response: Corrected.

(169) "whose upper part was scaled": what do you mean by "upper part"?

Response: Rephrased.

(170) "The three prescribed. . . profiles": This is confusing. Fig. 2 shows profiles labeled Kz, 0.1 Kz and 0.01 Kz, but here in the text you refer to 0.03 Kz and 0.001 Kz. Which is right? The figure legend or the text?

Response: Initially we used 1Kz, 0.1 Kz and 0.01 Kz, but then it turned out that 0.001 Kz is also interesting, so finally 1Kz, 0.03 Kz and 0.001Kz were used for the paper. The figure has been replaced now. Also line colors changed to agree with the rest of the paper.

(200) "the difference of equilibrium mixing ratio of SF6": How is this relevant in a range of pressure (0.1-0.2 hPa) where molecular diffusion is essentially negligible? The equilibrium profile defined by Eq. (5) is relevant for the upper mesosphere and above, which is beyond the upper boundary of the model used here. In fact, Eq. (5) and related discussion do not add anything useful to the problem of modeling SF6 below the lower mesosphere.

Response: We would not agree with the statement that molecular diffusion is always negligible below the mesosphere. The molecular diffusion is the key mechanism for gravitational separation which has been observed in stratosphere Ishidoya et al. (2008, 2013); Sugawara et al. (2018). As shown in Sec. 4.1, the effect of the gravitational separation on the AoA reaches a fraction of a year, which is comparable to the magnitude of corrections to the SF6-AoA considered e.g. by Stiller et al. (2012). The sensitivity studies indicate small but noticeable effect of molecular diffusion even for "1Kz". The molecular diffusion has little effect on the SF6 distribution due to the overwhelming impact of mesospheric depletion rather than due to the eddy diffusion. The latter result is worth including into the paper, in our opinion.

(203) "in the upper stratosphere heavy gases can no longer be considered as tracers and the molecular diffusion should be treated explicitly": I do not believe this is right. Molecular diffusion effects should be small compared to eddy mixing and mean meridional advection below the upper mesosphere (75-80 km), and certainly within the range of altitude of the present simulations (top boundary at 0.1 hPa, about 65 km).

Response: Since the gravitational separation occurs in the stratosphere, molecular diffusion should be accounted for in order to reproduce the separation.

(225) "flux decreased by several orders of magnitude . . . at the level of a few Pa": But in Fig. 3 all flux profiles increase with altitude. What is the definition of the flux shown in that figure? Does it not include a density factor?

Response: The plotted quantity is $\tilde{F}(p)$, which is defined as upward flux $F(p)$ [kg/m2] normalized with mass mixing ratio $\xi(p)$ [kg/kg] at each level. The statement is about the flux $F(p)$, which indeed vanishes as the destruction rate gets higher. In the revised version we use $F(p)/\xi(p)$ everywhere instead of $\tilde{F}(p)$.

(226) "shown in Fig. 3 with solid lines": Flux profiles in Fig. 3 are labeled Kz, 0.1Kz, 0.01Kz and 0.001Kz. Do these correspond to the Kz profiles of Fig. 2, except that 0.001Kz is not shown in that figure?

Response: Yes. Corresponding note added. The figures have been changed to same set of profiles.

(234) "For higher eddy diffusivity . . . molecular diffusion . . . becomes negligible": This should be the situation in the middle atmosphere up to about 75-80 km. Gravity wave parametrizations yield values of Kzz of order 10 m2 s-1 in the lower mesosphere (around 65 km); and mean vertical advection is also large at these altitudes. Therefore, for all practical purposes the effects of molecular diffusion and gravitational separation should be negligible over the range of altitude considered in this study. Note also that, according to Fig. 3, molecular diffusion effects are essentially irrelevant even for unrealistically weak values of eddy diffusion near the upper boundary (0.1 Kz and 0.01 Kz).

Response: We have to respectfully disagree. Molecular diffusion is the mechanism behind the gravitational separation. The effects of molecular diffusion on SF6 are negligible only because of the depletion. We are not aware of any earlier studies that explicitly quantify the effect of molecular diffusion on SF6 and apparent AoA, this, we believe that molecular diffusion is worth considering.

(246) "uppermost layer": What is the upper boundary condition on the circulation? Does it force the vertical velocity to be zero at the top boundary? If so, note that the effect of mean meridional transport on SF6 distribution and lifetime will not be modeled realistically.

Response: Yes, we force zero vertical velocity at 0.1 hPa. We put it more explicitly in Sec. 3. A note on mean meridional transport added to Discussion.

(265) "'ones' tracer": "unity tracer" might be better.

Response: The term replaced.

(304) "the southern polar region": What range of latitude does this cover?

Response: The corresponding note has been in the figure caption. Same duplicated in the text now.

(320) "inter-annual variability": This strongest variability seen in Fig. 4 is annual, presumably associated with the cycle of downwelling in winter and upwelling in summer. This again brings up the question what is the upper boundary condition on the dynamics (cf. comment at line 246), and how realistically mean vertical advection is modeled near the upper boundary. Note also that the mean meridional circulation in the mesosphere depends strongly on the contribution of gravity wave drag to the zonal-mean momentum budget, which would depend on how this is parameterized in the ERA-I reanalysis. Details on all of these points are needed.

Response: Note on annual variability added. Specification of the upper boundary condition added to "Model setup" section, and discussion of the resulting artifacts added to new "Discussion" section.

(324) "simulations with 0.01 Kz": Do you mean 0.001 Kz? That is what the legends in the left column panels of Fig, 4 indicate.

Response: The description was from the previous version of initialisation run, which was indeed made with 0.01 Kz. The new description is made more consistent.

(330) "molecular diffusion . . . maintains the upward flux . . . even if eddy diffusivity ceases": But in the real world, the flux at 65 km (0.1 hPa) is controlled principally by the combined effects of eddy diffusion and mean vertical advection.

Response: We put more clearly that the statement is about the model. The relation of the model to the real world is addressed in "Discussion" section.

(341) "vertical exchange is a key controlling factor": This is correct, but note again that flux due to mean vertical advection is also important and may or may not be modeled properly in the present study, depending on how the upper boundary condition is handled.

Response: The description of the upper boundary condition was clarified.

(357) "way and rate of SF6 destruction": What does "way of SF6 destruction" mean? You have varied the effective loss rate by changing the flux at the upper boundary, but as far as I can tell the loss mechanism was not changed.

Response: We meant that in the troposphere even difference in passive vs. non-passive SF6 is small. The statement rephrased.

(365) "the most diffusive case . . . overstated SF6": This is likely due to the fact that the "1 Kz" profile has too large values in the lower stratosphere (although it has more reasonable values in the upper stratosphere and lower mesosphere).

Response: Agree. The next sentence points exactly that. The discussion on how reasonable the profiles are has been added to "Discussion".

(373) "largest deviation below 20 km": See previous comment.

Response: Rephrased.

(375) "WACCM . . . under-representing the depletion of SF6 inside the polar vortex": The problem with the WACCM result is that the standard version of the model does not include loss due to electron attachment, only photolysis. I would expect WACCM to simulate SF6 quite accurately if all loss terms were included. What this result demonstrates is that it is essential to include loss via electron attachment.

Response: Thank you! Corresponding note has been added. We agree that "it is essential to include loss via electron attachment". However, comparison of our Fig. 7 to Fig. 3 from the next WACCM paper by Kovács et al. (2017) shows that just including loss via electron attachment into WACCM is not sufficient to reproduce the SF6 profiles in polar regions.

(386) "In all the above cases, the '1 Kz' profile is . . . too diffusive": I don't see this in all cases. The 1 Kz profile produces good agreement in the upper stratosphere in Fig. 6 b and d.

Response: Rephrased. Despite the modelled SF6 profiles for '1 Kz' are the closest to observed points above 25 km within the polar vortex, they fail to reproduce the shape of the profiles there.

(387) "The '0.03 Kz' profiles appear to be most realistic": Actually, none of the profiles is realistic. In particular, the range of Kzz as a function of altitude obtained from gravity wave parameterizations is much larger than shown for the 1 Kz profiles of Fig. 2, where Kz varies from a little under 1 m2 s-1 at 20 km to less than 10 m2 s-1 at 65 km. In models that include a gravity wave parameterization, Kzz is estimated to vary between less than 10-3 m2 s-1 and more than 10 m2 s-1 over the same range of altitude. For a recent example, see Zhu et al. (JAS, 67, 2520, 2010).

Response: The word "realistic" was meant for SF6 profiles rather than for Kz profiles. The statement rephrased. The Discussion on how (un-) realistic the Kz profiles has been added.

(432) "lack of a pole-to-pole circulation": Is this a result of the way the upper boundary condition is handled in these simulations? You need to show the Transformed Eulerian mean circulation as a function of altitude and latitude, at least for the solstice seasons, so the reader can understand the role of mean meridional transport near the top boundary of the model. Explicit description of how the upper boundary flux is handled in SILAM is also necessary.

Response: "lack of a pole-to-pole circulation" is a known feature of ERA-Interim reanalysis. The analysis of the mean circulation and distortions introduced by the "hardtop" diagnostics has been added to the paper. We compare the seasonal-mean diagnosed vertical velocity fields used for the run to the ones obtained from ERA5 meteorological dataset. For ERA5 "hardtop" was implemented at 10 Pa, to match one in our simulations and at 0.1 Pa to have a reference case.

(433) "understate it above 40 km": In this instance, one could also question the observations, especially the ones that show an increase in mixing ratio with altitude. It is unclear how such profiles could be generated for a tracer that has a source in the troposphere and a sink in the mesosphere.

Response: We agree, such behaviour is counter-intuitive and is probably related to the observational uncertainty. However, an intermittent increase of the mixing ratio with altitude is possible and could be noticed also in the model results, e.g. the SF6 shape of the non-collocated 0.001Kz profile at Fig. 6g of the revised manuscript.

(435) Figure 8: Is the "de-biased RMSE" in the figure caption the same thing as "STD" in the ordinate label of the top panel? It would be desirable to keep the terminology consistent to avoid confusion.

Response: Thank you! Replaced with "standard deviation of model-measurement difference".

(436) "the difference in statistical scores of the three selected simulations is quite minor": What "statistical scores" are you referring to?

Response: The scores (RMSE, bias and NMB) shown in the figures. The sentence has been rephrased.

(440) "standard deviation of model-measurement difference": How does this eliminate the influence of model bias, assuming that is what you mean to say here? Doesn't the model-measurement difference contain the bias? A formal definition of this quantity, similar to what is done in Eq. (11) for the NMB, would be useful.

Response: Definitions for standard deviation of model-measurement difference (STD) and absolute bias added, along with normalised mean bias (NMB).

(444) "RMS error of the observations due to retrieval noise in the original MIPAS data": Is this what you mean by the legend "MIPAS noise" in the top panel of Fig. 8?

Response: Yes. Note added.

(450) Figure 9: This needs labels for the various curves, as in Fig. 8.

Response: Corrected.

(452) "for the upper troposphere": What does this refer to? This paragraph discusses results for 30-60 km. What does this have to do with the upper troposphere?

Response: We meant the upper stratosphere. Misprint corrected.

(460) "Three other profiles of Kz result in practically identical distribution of AoA": This would imply that vertical mixing is irrelevant for the small Kz cases, and raises the question what controls AoA in these simulations.

Response: The AoA is controlled by the transport with explicitly resolved winds, which have a dominant effect unless the eddy diffusivity is too high. Corresponding note added.

(484) "The resulting model-based apparent AoA [is] much older than the "ideal-age" AoA and pretty close to the values derived from MIPAS": This is an important result that highlights the role of fast mesospheric destruction of SF6 due to the electron attachment mechanism.

Response: Thank you! The statement has been added to the Conclusions.

(503) "The reason is. . .": You should reference Stiller at al. (2012) here, who already pointed this out.

Response: The reference added.

(512) "'ideal age' and "passive" tracers: Are the results for the "ideal age" tracer the set of points labeled "time lag" in Figure 12? Again, consistency in terminology would be desirable.

Response: Corrected

(537) "eddy-diffusivity profile of Hunten (1975) scaled down": The Hunten profile almost certainly overestimates diffusivity in the lower stratosphere, but reducing it by a factor of 0.03 will not reflect the behavior of vertical mixing in the upper stratosphere and the mesosphere. Ideally, one would estimate vertical mixing (as a function of altitude, latitude and season) from a gravity wave parameterization. Since such a parameterization was not available in the context of the present study, the conclusions regarding the role of Kz in determining age of air cannot be taken at face value.

Response: We agree that proper parametrisation of eddy diffusivity would be more appropriate. The next sentence explicitly states that the conclusion is specific for our setup, and in the revised version we have tried to make it more clear. In the future we would be happy to implement some more realistic Kz scheme, that would use some physical parameters that govern the turbulence rather than just altitude, latitude and season.

Typos, etc.:

(28) "that presents an analogy of Lagrangian clock" -> "that is analogous to a Lagrangian clock"

(33) "are not possible, therefore. . ." -> "are not possible; therefore, . . ."

(285) "Eulerian analogy" -> "Eulerian analog"

(318) "is by more than an order of magnitude stronger than one of gravity separation"

-> "is stronger than diffusive separation by more than one order of magnitude"

(319) "Regardless the used Kz profiles" -> "Regardless of the Kz profiles used"

(344) "depleting SF6" -> "SF6 that undergoes chemical destruction"

(344) "start to fall down" -> "begin to decrease"

(452) "on pair" -> "on par"

(482) "nor its mixing ration" -> "nor does its mixing ratio"

Response: Thank you! Corrected accordingly.

2 Response to the Interactive comment RC2

The study by Kouznetsov et al investigates the impact of the vertical diffusion and of the mesospheric sink of SF6 and the SF6 climatology and its trends using a chemistry transport model. While the mesospheric transport is not explicitly included (due to lack of ERA-Interim data above 0.1 hPa), a parametrization of eddy diffusivity as well as molecular diffusivity is included to mimic transport to the mesosphere. The subject of the study is of high relevance, as SF6 is used frequently to estimate Age-of-Air, and the role of its sinks needs to be better understood. The study is overall well presented and the methods are overall appropriate, but some clarifications are needed (see comments below). Overall, I recommend the authors revise the paper minorly before it can be considered for publication.

General comments:

1. In lines 45 ff, you correctly mention that a correction has to be applied when deriving AoA from a non-linear increasing tracer, as SF6, as has been done by observational studies. However, it is not entirely clear to me how you calculated AoA from SF6 simply as time lag, as for the linear increasing tracer? It certainly is known that just calculating the time lag leads to deviations from the true AoA values. If you choose not to include a correction method in the calculation of AoA, you certainly should stress this fact, and I suggest you to refer to the SF6-derived "AoA" as "time lag" rather than AoA. The comparison of the SF6-derived time-lag with / without chemical sink is still valid, but I caution you on the conclusions you draw from the difference of the passive sf6 tracer and the ideal age /linearly increasing tracer: as long as no correction method for the non-linearity is implied, you cannot conclude on whether the non-linear increasing tracer can be used to deduce AoA values in general.

Response: We agree that the difference between "time lag" and AoA is influenced by the source variation and non-linear growth of concentrations. However, as shown by Waugh and Hall (2002), the "time lag" is a function of both the variation of surface concentration and the transient time distribution (TTD, also known as "age spectrum"). While the surface concentrations of SF6 are relatively well known, TTD is quite uncertain and can be only partially constrained with multi-tracer observations. Therefore, we believe that no fully-consistent correction to the "time-lag" AoA can be designed solely on SF6 distribution and non-linearity of its growth. Without this correction, the time lag is somewhat different from the mean age. The

"apparent age" however refers to the much larger problem of the strong SF_6 loss in the mesosphere and describes the fact that the age derived from SF_6 subsided from the mesosphere is much older than the realistic age. The corrections applied this-far in the literature do not address it. Throughout the paper, we refer to the SF_6-derived "AoA" as "apparent AoA", which is derived without any corrections. A paragraph has been added to the "AoA and apparent SF_6 AoA" section explicitly pointing it out and noting that our conclusions refer to this very quantity.

2. While the parametrizations of eddy diffusivity, gravitational separation by molecular diffusion and of SF6 loss are described well in detail, the way they are actually implemented in the model is not entirely clear to me. According to Section 3.4, the overall budget equation of the abundance of a tracer (SF6) is solved for steady state, and this steady state solution scaled by the actual tracer concentration is used above the model top - is this correct? And how exactly is this implemented - as loss due to the lifetime given in line 238 ? Furthermore, it was not clear to me whether the diffusive parametrizations are also applied in the actual model domain, or only for the parametrization above the top level? It could be helpful if you describe the overall approach at the beginning of section 3 (i.e. parametrization of upward transport above ∼10Pa by vertical diffusion, where SF6 is depleted, and thus there is no downward transport of SF6).

Response: The way the molecular diffusion is implemented has been described in the last paragraph of the "Molecular diffusivity and gravitational separation" section. The loss of SF6 through the domain top was implemented as a linear decay of SF_6 in the topmost model layer, at a rate derived from the $K_z(p)$ profile used in each simulation. This is now expressed more explicitly at the end of the "Parametrization for destruction of SF_6 in the mesosphere" section.

As it was stated in ll. 287-289 of the original submission, the runs were made with a set of eddy-diffusivity profiles and corresponding SF6 destruction rates in the topmost layer. The Kz was adjusted inside the model domain (ll 170-174 of the original submission). The statement in the last paragraph of the "model setup" section has been reformulated to make it more explicit that Kz was adjusted inside the model domain accordingly.

3. Related to the above comment, I wonder how sensitive your results are to the fact that you represent transport above the model top only as vertical diffusive process, i.e. the actual transport circulation is missing (which circulates air, and thus SF6 from pole-to-pole, as opposed to your assumption of all SF6 that is transported diffusively upward being lost). Probably the lack of advective transport also affects the results of the evaluation of different values for Kz? Or is this more based on the layers within the model domain (if diffusion is applied there too, see comment above)? Please add discussion of those issues to your study.

Response: The discussion of the effect of a hard "lid" for regular transport has been added. The current simulations indeed could not include the pole-to-pole circulation due to the limitations of ERA-Interim. However, as we showed, lifetime of SF6 quickly reduces starting practically from the top of our domain. Therefore, the impact of the missing topmost layers is bound to be limited, mainly reducing the SF6 concentrations in the downdraft regions: there is little SF6 above 60 km.

Specific comments: - line 25: you describe here the estimation of AoA with Lagrangian trajectories, but without inter-parcel mixing. The inter-parcel mixing does affect AoA, and there are studies that account for this mixing in Lagrangian frameworks (e.g. Brinkop and Jöckel, 2019; Plöger et al., 2015b) Thus estimates of AoA with Eularian methods might differ

from Lagrangian methods due to the way inter-parcel mixing is calulated. This methodological point should be mentioned somewhere.

Response: References added, the role of mixing is emphasised.

- line 27: "above-mentioned observational method": I dont see you mention the observational method above this statement?

Response: Corrected

- line 44: Garcia et al did show that the corrections improve the trend estimate, and they do not use the exact same correction method than what was applied to the observations. So I would not argue that the tracers are "ambiguous proxies" for AoA, but rather that the correction methods accounting for the non-linearity need to be investigated more deeply.

Response: Garcia et al. argue that corrections would need a knowledge of age spectra in order to estimate a mean age. The corrections we are aware of (e.g. Stiller et al., 2012) are based on the assumed shape of age distribution and validity of a world constant of $w = 0.7\,\mathrm{year}$ that describes the broadening of the spectra. One of the goals of the paper is to show that there are more direct and more accurate ways of computing AoA without involving such corrections. We added discussion of the corrections to "discussion" section.

- line 95 ff: Maybe you can mention here which variables from ERA-Interim you use - I was wondering at this point how vertical transport is calculated, and this became clear only in section 3.5.

Response: List of variables and ref to Sec. 3.5 added.

- line 122 ff, general: How certain are the SF6 destruction rates, i.e. how do the results by Totterdill et al compare to other studies? Please add a short statement.a

Response: Added. Intriguingly enough, IPCC (2013, Sec 8.2.3.5) states that photolysis is the main destruction mechanism without references. Totterdill et al. (2015) says:"Photolysis is currently recognized as the major sink of SF6 (Ravishankara et al., 1993), though with a significant contribution from electron attachment in the upper mesosphere and lower thermosphere (Reddmann et al., 2001)." However (Reddmann et al., 2001) clearly shows the dominant role of the electron attachment below 80 km.

- line 156: its not clear to me what the "limiting value" is, and why Kz is "practically always" set to it? Please be more specific here.

Response: The sentence discarded as redundant. It was supposed to stress the idea that ECMWF scheme is equivalent to zero-Kz in the stratosphere.

- line 159: Kz does not fall below the molecular diffusivity in the lower stratosphere, below ∼40 km, according to Fig. 2, so please refine the statement.

Response: Rephrased.

- line 196: do you mean mixing ratio differences between the two layers? Why two layers, and not at one layer? Or do you mean the mean mixing ration in the layer bounded by an upper and lower pressure? it might be easier to put down the equation rather than describing it.

Response: Thank you! The equation is indeed more clear.

- line 212: I assume you use the US standard atmosphere because at the levels where it matters, ERA-Interim is not available any more? Again, it is not entirely clear if / how you apply this parametrization only at the "top layer", or also throughout the model domain. If the latter is true, the actual ERA-Interim temperatures could be used in the model domain (even tough you could argue that it does not make much of a difference there, as molecular diffusion does not play a role).

Response: We use standard atmosphere because it allows for pre-calculating a single set of exchange coefficients for a given species and vertical discretisation. The coefficients applied throughout the domain with a simple explicit scheme. The paragraph rephrased to emphasise this.

- line 224: please be more specific and describe how you obtain the flux F(p) from the steady-state solution of the mixing ratios.

Response: Rewritten. The requested details added.

- line 236: see general comment: please be more specific on how exactly the different parametrizations are used in the different areas, and how the upper boundary parametrization is implemented (via the lifetimes?)

Response: Yes. Note added at the end of the "model setup" section.

- line 250: which "other parameters" do you use?

Response: Surface pressure, temperature and humidity. Note added.

- line 267: were the other tracers corrected using the "ones" tracer, or just the error "evaluated"?

Response: Yes. Note added.

- line 343 ff: is this the best way to estimate lifetimes, or couldn't you just average the inverse destruction rate mass-weighted over the entire atmosphere?

Response: Yes. Corresponding note has been added.

- Also, at line 348, you write that the delay of SF6 between troposphere and upper layers is about 5-6 years, and then use the value 5 years previous to the emission stop to evaluate the lifetime - is this quantitative, or just a rough estimate?

Response: 5-6 years is an estimate of AoA in the topmost model layer. Corresponding note added.

- line 361: "we have found in literature"-> be more specific, e.g. observations that were published by ...

Response: The references duplicated from the figure caption.

- line 365: "strong exchange through the troposphere"? do you mean too strong upward transport by the diffusion?

Response: Yes. Thank you!

- line 384: what is the dynamical reason for the minimum in SF6, and why do you think it is weaker in the model?

Response: The minimum is a result of the spring breakdown of the polar vortex, when a regular down draught ceases, and atmospheric layers decouple from each other. The reduced depth of the modelled minimum is probably caused by insufficient

decoupling of the layers in the driving meteorology. Since we make an offline modelling, driving meteorology is a usual suspect. Corresponding note added.

- line 464: "practically"? please be more specific

Response: The sentence was about SF6 profiles rather than Kz profiles. Rephrased.

- line 471 ff: as mentioned in the general comment, you should clarify how AoA was calculated from the SF6 tracers, and possibly change the naming to "time-lag".

Response: A note on the method added. As AoA derived from passive Eulerian tracers is a time lag by definition, adding "time-lag" would be probably redundant in this case.

- line 486: you mentioned earlier that you use a new version of the MIPAS SF6 data, but do not show its AoA, but instead refer to the older published AoA figures. Why don't you add the new MIPAS AoA to Figs. 11 and 12?

Response: Figs. 11 and 12 show average model fields. As it is shown in Fig. 7, average of sampled fields differs noticeably from the "true" average. Adding observational data would require model data to be sampled according to observation timings and averaging kernels, which would change the message of the figures. Their purpose is rather to show, how sensitive AoA and estimated trends can be to the choice of particluar method to infer it. For that, we need full model output without down-sampling to the satellite overpasses.

- line 515: "non-uniformity" of ERA-Interim, what do you mean? Couldn't this just be the trend in AoA over the period, or why do you think it is an artefact? Further, in line 519, you state that ERA-Interim was not recommended for climatological studies. I'm surprised by this statement, given that ERA-Interim is the basis for a lot of studies of climatologies and trends in various variables. Can you specify which source you quote here, and what exactly should not be done?

Response: Figures 21 and 22 of Dee et al. (2011) indicate a clear impact of the inhomogeneous assimilated data set on analysis increments. We have found similar features in the simulated ideal-age AoA. The main reason for the inhomogeneity in the ERA-Interim data is varying amount of observations from year to year, as shown by ?????Dee et al????????. Excluding artefacts caused by changes in the amount of the observational information would require extensive effort and an independent homogeneous dataset, which does not exist for AoA. Deducing reliable trends even for atmospheric temperature, quantity that is directly and indirectly measurable and has been extensively assimilated throughout the whole ERA period, was a major effort (Simmons et al., 2014). Therefore, we are sceptical on mere possibility of deducing reliable trends for AoA using ERA-Interim alone.

- line 521: The trends over the MIPAS period could be compared to other CTM results, e.g. by Plöger et al. (2015a), who showed that their CTM was capable to reproduce the MIPAS AoA trend rather well.

Response: The reference and discussion of the differences added.

- line 525: why comparable with Lagrangian simulations? As pointed out before, one difference is the accounting for inter-parcel mixing. I'd rather argue that your results are comparable to other state-of-the-art CTM simulations of AoA.

Response: Thank you! Corrected.

- line 542: Are those "best" estimates in the upper stratosphere based on the "upper layer", where advective transport is not accounted for? Or do you refer to the results in the model domain?

Response: We refer to the results in the model domain. Remark added.

-line 549: I dont understand the sentence on the standard deviation controlled by noise. Do you mean to say that the standard deviation between model and MIPAS is about as large as the error on the satellite data?

Response: Yes. The remark added.

- line 551: you might want to add the range of lifetimes you obtain.

Response: Added.

- line 560: as stated in the general comments, as long as you do not apply corrections for the non-linear growth, you can not conclude on the suitability of the non-linear tracers in general. You can conclude here that without correcting for the non-linear growth, the apparent AoA and its trends deviate strongly, and that this motivates the investigation of correction methods.

Response:

We agree, that one could more-or-less compensate for the non-linear growth. The main issue with SF6 age is the mesospheric sink, that can hardly be compensated. The statement has been rephrased to make it more explicit.

Typos/ Language / Technical:

- Abstract, line 11: ".. does not exceed 6-6.5 years": it is not clear to me what this statement refers to - is this the "true" (ideal age) maximum value for AoA?

- line 18: what do you mean by "polar circulation" ?

- line 37, and general: check the parenthesis around references, they are incorrect at several places, for example here it should read (Waugh, 2009 ; Stiller et al., 2012)

Response: Corrected

- line 86: "transformation procedure" - do you mean the chemical "transformation"? -> change to "chemical sinks" (?)

Response: We mean both sink of SF6 and the increment of “ideal age”, and also molecualr diffusion for SF6. “corresponding transformation and transport routines” is hopefully less ambiguous.

- line 122: over 60 km -> above 60 km; "that fall..." -> "i.e. within and above the top most..."

Response: Nominal top of the ERA-Interim (topmost half-level) is at the top of the atmosphere.

- line 159: please avoid using the word "practically", as it is not very specific

Response: Removed/replaced.

- line 168: "than ones accepted.."- Do you mean "than the ones usually used in models"?

- line 176: "the mesosphere" (add the)

- line 196: "in the vertical, one obtains that the ..."

- line 202: the overwhelming" (add "the")

- line 247: remove "been"

- line 267: "rations" -> "ratios";

- line 300: "downdraught" -> "downwelling"

- line 344: fall down -> decrease

- line 383: "the one in Fig.." (add the)

- line 386: "furthermost" -> furthest

- line 419: to the polar (replace "a" by "the")

- line 426: overstating -> overestimating

- line 452: do you mean upper stratosphere?

- line 482: "nor its ..."-> "nor does its mixing ratio" (remove "n")

- line 484: replace second "well" with "with"

- line 490: pointed out (add "out")

Response: Thank you! Corrected.

3 Response to the Interactive comment RC3

This is an interesting manuscript exploring, in a model environment, the effects of chemistry, gravitational separation and diffusivity on SF6 mixing ratios in the stratosphere and the mean age of air derived from it. Clearly a lot of work has gone into devising the various model setups and I would in general support the publication of this work. However, some questions need to be answered and some potential issues resolved beforehand. One example is e.g. that even though it is driven by ERA-Interim there is no guarantee that this model will accurately reproduce stratospheric transport patterns including the overturning circulation, transport barriers, the QBO, etc., all of which can influence AoA. Perhaps this was demonstrated in Sofiev et al., 2015? If so, it would be good to give a short summary, if not, some further details are required. Some further points can be found in the below.

Response: Sofiev et al., 2015 describes the transport procedure used in SILAM without touching any specific meteorological driver. ERA-Interim until recently had been a State-of-the-Art reanalysis which has been evaluated in many studies. The purpose of the present study was not to analyse in details how well the particular phenomena are reproduced by ERA-Interim, but rather to simulate SF6 evolution and distribution simultaneously with other AoA-related quantities, and see how well SF6 and AoA can be reproduced within a single model run and whether their errors are correlated. Moreover, quite a few findings of the study are valid regardless the quality of the meteorological driver. Particular features of ERA-Interim and its interfacing to SILAM are considered only as long as it is necessary for the main topic of the paper. .

Title: Consider adding "the" before "distribution" and "SILAM". There are various other places in the manuscript with small language deficiencies like this.

Response: Corrected

Abstract: An introductory sentence to alert the reader to the fact that this paper is on the stratospheric overturning circulation (and perhaps its importance) would be helpful.

Response: We have tried to focus more on physical processes controlling SF6 concentrations in a given velocity field, and a way to simulate it, without getting into too much details about stratospheric circulation in general.

Line 11: This should be "adds" and I would also recommend adding "up to".

Response: Rephrased.

Line 32-33: Age is not the correct term here as oceanic water has been around for some time. I suggest replacing it with e.g. "transport times".

Response: Corrected

Line 109-113: I was quite surprised to find a new satellite product hidden in this modelling-focused manuscript. Given that there are "considerable" differences to previously published SF6 data sets I urge the authors to provide more details and make their statements more quantitative (e.g. defining "considerably higher" and "closer"; where does the "new" CFC-11 band come from?; does the correction influence trends in the 2002-2012 period?), perhaps even by adding a figure to support their claims.

Response: The SF_6 data used in this paper are retrieved following the procedure described by Haenel et al. (2015). The only difference to the latter dataset is the use of newly provided spectroscopic information. SF_6 mixing ratios are up to 0.6 pptv higher in the upper stratosphere above 35 km, with main differences in the tropics and the polar regions. This brings AoA above 25 km in close agreement with reference balloon data as shown in Waugh and Hall (2002). The AoA trends change on detail level, however the general pattern with increasing AoA in the NH and decreasing AoA in the tropics an SH remains. A paper on the differences between the new and the Haenel et al. version is in preparation (Stiller, G.P., J.J. Harrison, F.J. Haenel, N. Glatthor, S. Kellmann, N.N., Improved global distributions of SF_6 and mean age of stratospheric air by use of new spectroscopic data, to be submitted to Atmos. Chem. Phys.). Similarly, a paper on the laboratory measurements of the SF_6 absorption cross sections is in preparation by J.J. Harrison. The "new" CFC-11 band in the spectral vicinity of the SF_6 spectral signature is described in Harrison (2018)

Line 118-119: Figure 1 is bad quality and Figure 2 needs some further explanation in the caption.

Response: Figure 1 is an attempt to plot the parametrisation over the original graphics from Totterdill et al. (2015, Fig. 9). Caption of Figure 2 extended.

Line 119: Is it Silam or SILAM?

Response: SILAM is used through the manuscript now. Backronym introduced.

Line 170-171: Looking at Figure 2 none of the three profiles seem to capture the vertical gradient from the ERA-5 data. Why is that?

Response: The ERA5 Kz profile is below the molecular diffusivity. Thus we have more questions to the order of magnitude than to the gradient. Investigating the physical reasoning behind the ERA5 profiles is definitely worth the effort, we plan it for the next study.

Line 219-220: Please quantify: How negligible does vertical advection need to be? And how does that compare to actual vertical advection in the stratosphere and mesosphere?

Response: Brief note on the magnitude of vertical advection added. The comparison to the magnitude of the vertical advection in ERA5 added to the discussion section.

Line 259: The details of the simulation setup are beyond my expertise. However, this statement seems somewhat vague. What does "normally" mean here? And how large is the precision of the input wind fields? Does it e.g. vary over time?

Response: The precision is a feature of the way the fields are encoded. More specific figure added.

Line 273-275: This is a major problem. A linear extrapolation can introduce biases, especially since 4 years of the extrapolated period overlap with the MIPAS period. Why do the authors not use more up-to-date publically available data, e.g. from the AGAGE and NOAA ESRL networks. Looking at Figure 1-21 in the recent Scientific Assessment of Ozone Depletion (2018), global emissions of SF6 appear to have been much lower between 2008 and 2016, closer to 0.21 Gg/yr. The implications for the derived AoA and its trend could be quite severe and should at least be assessed.

Response: Thank you for the reference. Corresponding note and citation added. The difference is about 7% of annual total emission by 2016, which is comparable to the uncertainty range shown in Fig 1-21 of Engel et al. (2018). The difference is certainly worth accounting in follow-up studies, but we do not see how it could noticeably affect the results of the present study.

Line 287-294: This paragraph raises a few questions. What does "0.001Kz eddy diffusivity" mean in detail and why was the initialisation performed that way? When was the initialisation started? Which emissions were used for SF6 species from 1980-1989 and which meteorological fields for 1970-1979? What about the pre-1970 time period?

Response: The description has been corrected with more details provided.

Line 306: This should be "from".

Response: Corrected

Line 313-314, 353-355: Why are the lifetimes in Table 1 so long? It looks like the model is not able to reconcile realistic diffusion rates with recently published lifetime estimates for SF6 (e.g. Kovacs et al. and Ray et al.). This needs to be discussed. I also do not agree that there is good agreement with lifetime estimates from other studies (Line 353-355) as all of the higher lifetime estimates ($\gtrsim$ 1500 years) come from outdated studies.

Response: We are not so certain about the over-estimation in the older studies and whether the shorter lifetime is a evidence-based consensus now. For instance, the model of Kovács et al. (2017) overstates the SF6 content in the altitude range of 25 – 50 km (compare Fig. 3 there to the Fig. 7 of the manuscript). It should lead to enhanced transport of SF6 towards the depletion layers and thus overstate the destruction rate and underestimate the lifetime. The estimate of Ray et al. (2017) is

based essentially on a single observed profile of SF6. The subsection is moved after the SF6 evaluations, and corresponding discussion added.

Line 399-400: Please improve Figure 7. It is currently very hard to decipher the legend and text inside the graph area and the two lines for each colour are undistinguishable.

Response: The legend has been moved to the upper-right panel. The thin lines made also dashed and the grid made light-grey. Hopefully, the figure is more readable now.

Also, please add the uncertainties of the MIPAS data points (one could at least add standard deviations of the observed values as in Kovacs et al.) and why are SF6 mixing ratios increasing at the high altitude end for some profiles?

Response: The uncertainties added. The note on non-monotonous profiles added.

Line 471-475: Plotting the residual between 11a,b and c might help visualising the differences. Also, please quantify "slight old bias".

Response: Colors are indeed difficult to compare. The shape of the isolines, however seems to visualize it quite well. "slight old bias" replaced with more specific "old bias up to 3-5 months".

Line 547-548: Looking at Figure 7 I cannot agree with this statement, at least not until some realistic uncertainty estimates have been added to the observations.

Response: All but one balloon data sets come without uncertainties. Mipas uncertainties added. The satement rephrased.

Line 551-552: This is right at the upper end of recent estimates, so not too good agreement. Given that the authors state themselves earlier in the manuscript that "insufficient vertical resolution of ERA-Interim in the upper stratosphere and lower mesosphere, and lack of pole-to-pole circulation" limit model performance (resulting also no conclusion being drawn on AoA trends) I find that statement too strong.

Response: The word "good" removed. Also see the notes at the end of the "Lifetime…" section.

Page 28-29: Figure 8 and 9 are currently not mentioned anywhere in the manuscript.

Response: They were discussed and referenced in lines 434 – 453 of the original submission.

4 Response to the Interactive comment RC4

This paper simulates the impact of the mesospheric destruction and gravitational separation on stratospheric SF6 distribution using a chemical transport model driven by ERA-Interim meteorology. In the model, mesospheric depletion and gravitational separation of SF6 are parameterized as upper boundary conditions. Sensitivity simulation were conducted and the roles of mesospheric destruction, gravitational separation, and vertical turbulent diffusion in the distribution of stratospheric SF6 are determined. The effects of these processes on the derived mean age of air and its trend are also discussed. This paper clearly demonstrate that the apparent mean age of air derived from SF6 measurements is not suited for studying the trend of

stratospheric mean age of air. The results have important implications in understanding the differences in the observed and modeled Brewer-Dobson circulation trends. I recommend publication of the paper after my comments are addressed.

Comments: My major concern is that the SILAM model doesn't capture the SF6 distribution in the upper stratosphere. The authors attribute this deficiency to the low top of ERA-interim that can't accurately represent the circulation in the upper stratosphere and mesosphere. However, the mesosphere circulation, particularly the downwelling branch of the summer-to-winter pole circulation, is essential to understand how the mesospheric sink affects SF6 distribution in the stratosphere. This issue needs to be discussed in more detail. I wonder if it is possible to drive SILAM with a model of higher top, e.g., WACCM, to see if SF6 in the upper stratosphere can be improved.

Response: Yes. It is possible to drive SILAM with other models. It is in our plans to repeat the exercise with ERA5 once this publication has been complete. Such simulation would be possible to do with more rigorous handling of depletion, since ERA5 covers the depletion layers quite well. The processes are still to be implemented, however.

As an illustration on how the low-top affects the circulation we have added a comparison of the mean vertical transport in SILAM driven with ERA-Interim to the one driven with ERA5.

Section 5: Describe how the mean age of air is derived using SF6.

Response: The procedure described in the beginning of the section 5.2, together with a brief rationale behind the choice of the method.

Lines 484-486: Figure 7 shows that the simulated SF6 distribution doesn't agree with MIPAS measurement about 40 km (above 30 km in the winter pole). How can the derived AoA agrees with each other?

Response: The agreement is rather qualitative: both SILAM and MIPAS indicate over 10-years-old air in the upper polar stratosphere, which is way above the "ideal-age" estimates. The sentence has been reformulated.

References

Brinkop, S. and Jöckel, P.: ATTILA 4.0: Lagrangian advective and convective transport of passive tracers within the ECHAM5/MESSy chemistry–climate model, Geoscientific Model Development, 12, 1991–2008, 2019.

Dee, D. P., Uppala, S. M., Simmons, A. J., Berrisford, P., Poli, P., Kobayashi, S., Andrae, U., Balmaseda, M. A., Balsamo, G., Bauer, P., and et al.: The ERA-Interim reanalysis: configuration and performance of the data assimilation system, Q. J. Roy. Meteorol. Soc., 137, 553–597, https://doi.org/10.1002/qj.828, 2011.

Engel, A., Rigby, M., Burkholder, J., Fernandez, R., Froidevaux, L., Hall, B., Hossaini, R., Saito, T., Vollmer, M., and Yao, B.: Update on Ozone-Depleting Substances (ODSs) and Other Gases of Interest to the Montreal Protocol, Chapter 1 in Scientific Assessment of Ozone Depletion: 2018, Report 58, World Meteorological Organization, Geneva, Switzerland, https://www.esrl.noaa.gov/csd/assessments/ozone/2018/, 2018.

Harrison, J. J.: New and improved infrared absorption cross sections for trichlorofluoromethane (CFC-11), Atmospheric Measurement Techniques, 11, 5827–5836, https://doi.org/10.5194/amt-11-5827-2018, 2018.

IPCC: Climate Change 2013: The Physical Science Basis. Contribution of Working Group I to the Fifth Assessment Report of the Intergovernmental Panel on Climate Change, Cambridge University Press, Cambridge, United Kingdom and New York, NY, USA, https://doi.org/10.1017/CBO9781107415324, www.climatechange2013.org, 2013.

Ishidoya, S., Sugawara, S., Morimoto, S., Aoki, S., and Nakazawa, T.: Gravitational separation of major atmospheric components of nitrogen and oxygen in the stratosphere, Geophysical Research Letters, 35, https://doi.org/10.1029/2007gl030456, 2008.

Ishidoya, S., Sugawara, S., Morimoto, S., Aoki, S., Nakazawa, T., Honda, H., and Murayama, S.: Gravitational separation in the stratosphere–a new indicator of atmospheric circulation, Atmospheric Chemistry and Physics, 13, 8787–8796, 2013.

Kovács, T., Feng, W., Totterdill, A., Plane, J. M. C., Dhomse, S., Gómez-Martín, J. C., Stiller, G. P., Haenel, F. J., Smith, C., Forster, P. M., García, R. R., Marsh, D. R., and Chipperfield, M. P.: Determination of the atmospheric lifetime and global warming potential of sulfur hexafluoride using a three-dimensional model, Atmospheric Chemistry and Physics, 17, 883–898, https://doi.org/10.5194/acp-17-883-2017, 2017.

Plöger, F., Abalos, M., Birner, T., Konopka, P., Legras, B., Müller, R., and Riese, M.: Quantifying the effects of mixing and residual circulation on trends of stratospheric mean age of air, Geophysical Research Letters, 42, 2047–2054, https://doi.org/10.1002/2014GL062927, 2015a.

Plöger, F., Riese, M., Haenel, F., Konopka, P., Müller, R., and Stiller, G.: Variability of stratospheric mean age of air and of the local effects of residual circulation and eddy mixing, J. Geophys. Res. (Atmospheres), 120, 716–733, https://doi.org/10.1002/2014JD022468, 2015b.

Ravishankara, A., Solomon, S., Turnipseed, A., and Warren, R.: Atmospheric lifetimes of long-lived halogenated species, Science, 259, 194–199, 1993.

Ray, E. A., Moore, F. L., Elkins, J. W., Rosenlof, K. H., Laube, J. C., Röckmann, T., Marsh, D. R., and Andrews, A. E.: Quantification of the SF6 lifetime based on mesospheric loss measured in the stratospheric polar vortex, Journal of Geophysical Research: Atmospheres, 122, 4626–4638, https://doi.org/10.1002/2016JD026198, 2017.

Reddmann, T., Ruhnke, R., and Kouker, W.: Three-dimensional model simulations of SF6 with mesospheric chemistry, Journal of Geophysical Research: Atmospheres, 106, 14 525–14 537, https://doi.org/10.1029/2000JD900700, 2001.

Simmons, A., Poli, P., Dee, D., Berrisford, P., Hersbach, H., Kobayashi, S., and Peubey, C.: Estimating low-frequency variability and trends in atmospheric temperature using ERA-Interim, Quarterly Journal of the Royal Meteorological Society, 140, 329–353, https://doi.org/10.1002/qj.2317, 2014.

Stiller, G. P., von Clarmann, T., Haenel, F., Funke, B., Glatthor, N., Grabowski, U., Kellmann, S., Kiefer, M., Linden, A., Lossow, S., and Lopez-Puertas, M.: Observed temporal evolution of global mean age of stratospheric air for the 2002 to 2010 period, Atmos. Chem. Phys., 12, 3311–3331, https://doi.org/10.5194/acp-12-3311-2012, 2012.

Sugawara, S., Ishidoya, S., Aoki, S., Morimoto, S., Nakazawa, T., Toyoda, S., Inai, Y., Hasebe, F., Ikeda, C., Honda, H., et al.: Age and gravitational separation of the stratospheric air over Indonesia, Atmospheric Chemistry and Physics, 18, 1819–1833, 2018.

Totterdill, A., Kovács, T., Gómez Martín, J. C., Feng, W., and Plane, J. M. C.: Mesospheric Removal of Very Long-Lived Greenhouse Gases SF6 and CFC-115 by Metal Reactions, Lyman-α Photolysis, and Electron Attachment, The Journal of Physical Chemistry A, 119, 2016–2025, https://doi.org/10.1021/jp5123344, 2015.

Waugh, D. W. and Hall, T. M.: Age of stratospheric air: Theory, observations, and models, Reviews of Geophysics, 40, https://doi.org/10.1029/2000rg000101, 2002.

Simulating age of air and the distribution of SF_6 in the stratosphere with the SILAM model

Rostislav Kouznetsov[1,2], Mikhail Sofiev[1], Julius Vira[1,3], and Gabriele Stiller[4]

[1]Finnish Meteorological Institute, Helsinki, Finland
[2]Obukhov Institute for Atmospheric Physics, Moscow, Russia
[3]Cornell University, Ithaca, NY, USA
[4]Karlsruhe Institute of Technology, Karlsruhe, Germany

Correspondence: Rostislav Kouznetsov (Rostislav.Kouznetsov@fmi.fi)

Abstract. The paper presents a comparative study of age of air (AoA) derived with several approaches: a widely used passive tracer accumulation method, the SF_6 accumulation, and a direct calculation of an "ideal age" tracer. The simulations ~~have been~~ were performed with the Eulerian chemistry transport model SILAM driven with the ERA-Interim reanalysis for 1980-2018.

The Eulerian environment allowed for simultaneous application of several approaches within the same simulation, and interpretation of the obtained differences. A series of sensitivity simulations revealed the role of the vertical profile of turbulent diffusion in the stratosphere, destruction of SF_6 in the mesosphere, as well as the effect of gravitational separation of gases with strongly different molar masses.

The simulations reproduced well the main features of the SF_6 distribution in the atmosphere retrieved from the MIPAS satellite instrument. It was shown that the apparent very old air in the upper stratosphere derived from the SF_6 profile observations is a result of destruction and gravitational separation of this gas in the upper stratosphere and mesosphere. ~~The effect of these processes add over 4 years to the actual~~ These processes make the apparent SF_6 AoA in the stratosphere several years older than "ideal-age" AoA, which, according to our calculations, does not exceed 6-6.5 years.

The destruction of SF_6 and varying rate of emission make ~~it unsuitable to reliably derive~~ SF_6 unsuitable for reliably deriving AoA or its trends. However, observations of SF_6 provide a very useful means for validation of stratospheric circulation in a model with properly implemented SF_6 loss.

1 Introduction

AoA is defined as the time spent by an air parcel in the stratosphere since its entry across the tropopause (Li and Waugh, 1999; Waugh and Hall, 2002). The distribution of the age of air (AoA) is controlled by the global atmospheric circulations, first of all, the Brewer-Dobson and the polar circulation. In particular, the temporal variation of AoA has been used as an indicator of long-term changes in the stratospheric circulation (Engel et al., 2009; Waugh, 2009). AoA has been extensively used to evaluate and compare general circulation and chemical transport models in the stratosphere (Waugh and Hall, 2002; Engel et al., 2009).

Simulations of the AoA according to the definition above have been performed with Lagrangian transport models~~(Eluszkiewicz et al., 200~~. The trajectories are initiated with positions distributed in the stratosphere and integrated backwards until they cross the

tropopause. The time elapsed since the initialization is attributed as age of air at the point of initialization. Moreover, the distribution of the ages of particles originating from some location can be used to get the age spectrum there. Until recently Lagrangian simulations of AoA did not explicitly account for turbulent mixing in the stratosphere (Eluszkiewicz et al., 2000; Waugh and Ha . The account for mixing adds up to two years to the mean AoA in tropical upper stratosphere (Garny et al., 2014). In Lagrangian formulation the mixing can be simulated with random-walk of particles (Garny et al., 2014), or by inter-parcel mixing (Plöger et al., 2015; Brinkop and Jöckel, 2019).

The Eulerian simulations of AoA can be formulated in several different ways. The approaches with an accumulating tracer, ~~mimicking the above-mentioned observational method~~ whose mixing ratio increases linearly in the troposphere, were used in a comprehensive study by Krol et al. (2018) and several studies before (e.g. Eluszkiewicz et al., 2000; Monge-Sanz et al., 2012). Another approach is to simulate a steady distribution of a decaying tracer, such as ^{221}Rn, emitted at the surface at a constant rate (Krol et al., 2018). Besides that, a special tracer that ~~presents an analogy of~~ is analogous to a Lagrangian clock has been used. The tracer appears in literature under names "clock-type tracer"(Monge-Sanz et al., 2012) or "ideal age" (Waugh and Hall, 2002). The ideal age has constant rate of increasing of mixing ratio everywhere, except for the surface where it is continuously forced to zero. Similar tracers have been long used to simulate ~~age~~ transport times of oceanic water (e.g. England, 1995; Thiele and Sarmiento, 1990).

Direct observations of the age of air, as it is defined above, are not possible~~,~~ ; therefore AoA is usually derived from observed mixing ratios of various tracers. The tracers belong to one of two types: various tracers with known tropospheric mixing ratios and lifetimes (Bhandari et al., 1966; Koch and Rind, 1998; Jacob et al., 1997; Patra et al., 2011), and long-living tracers with known ~~trends~~ variations in tropospheric mixing ratios. The studies published to-date used carbon dioxide CO_2 ~~(Remsberg, 2015)~~(Andrews et al., 2001; Engel et al., 2009), nitrous oxide N_2O (Boering et al., 1996; Andrews et al., 2001), sulphur hexafluoride SF_6 ~~Waugh (2009); Stiller et al. (2012)~~(Waugh, 2009; Stiller et al., 2012), methane CH_4 ~~(Remsberg, 2015)~~ (Andrews et al., 2001; Remsberg, 2015), and various fluorocarbons (Leedham Elvidge et al., 2018).

For accumulating tracers~~a~~ , the mean AoA at some point in the stratosphere is calculated as a lag between the times when a certain mixing ratio is observed near the surface and at that point. The lag time is equivalent to the mean AoA defined above only in the case of a strictly linear growth and uniform distribution of the tracer in the troposphere (Hall and Plumb, 1994).

In reality, there is no tracer whose mixing ratio in the troposphere grows strictly linearly. The violation of assumption of the linear growth leads to biases in the resulting AoA distribution and its trends. It has been pointed out that increasing growth rates of CO_2 and SF_6 lead to a low-bias of AoA and its trends, and make these tracers ambiguous proxies for AoA (Garcia et al., 2011). Various corrections have been applied in several studies (Hall and Plumb, 1994; Waugh and Hall, 2002; Engel et al., 2009; Stiller et al., 2012; Leedham Elvidge et al., 2018) to deduce the "true" AoA from observations of tracers with increasing growth rates. The effect of the correction method on AoA estimates has not been investigated and must be considered as source of uncertainty in resulting estimates (Garcia et al., 2011). Garcia et al. (2011) further conclude that accounting for the biases in trend estimates due to varying growth rates would likely require uniform and continuous knowledge of the evolution of trace species, which is not available from any existing observational dataset. Recently Leedham Elvidge et al. (2018) have shown a minor sensitivity of AoA to the choice of particular correction method, however without detailed analysis of assumptions

behind these methods. For a similar problem with ages of oceanic water it has been shown (Waugh et al., 2003) that in case of a non-linearly varying tracer the tracer age is strongly influenced by the shape of transient time distribution (TTD, also known as an "age spectrum") at particular location and time.

Another major source of uncertainty in observational AoA is violation of conservation of a tracer due to sources and sinks, such as oxidation of carbon monoxide and methane for CO_2, or mesospheric destruction for SF_6. The mesospheric sink of SF_6 leads to an "over-aging", especially pronounced in the area of polar vortices. The magnitude of the over-aging was estimated as 2 or more years Waugh and Hall (2002). Besides being visible in many evaluations, e.g. Stiller et al. (2012, Fig. 4), Kovács et al. (2017, Fig. 8), a dedicated study on the over-aging of polar winter stratospheric air was performed by Ray et al. (2017, Fig. 4) .

The simulations of SF_6 and AoA in the atmosphere with WACCM model (Kovács et al., 2017) have reproduced the effect of over-aging, but of much smaller magnitude than if inferred from SF_6 retrievals from the limb-viewing **MIPAS** instrument operated on-board of the Envisat satellite in 2002-2012 (Stiller et al., 2012), and *in-situ* observations from the ER-2 aircraft (Hall et al., 1999). Kovács et al. (2017) offered two possible scenarios for the discrepancy: either SF_6 loss is still underestimated in WACCM, or MIPAS SF_6 is low biased above $\sim 20\,\mathrm{km}$. Neither of the scenarios have been analysed in depth so far, which leaves the status of MIPAS, the richest to date observational dataset for the stratospheric SF_6, unclear.

The aim of the present study is to provide ~~consistent simulations simultaneously reproducing the~~ self-consistent simulations of spatio-temporal distribution of AoA and of the SF_6 mixing ratio in the troposphere and stratosphere during last 39 years. The main modelling tool is the Eulerian chemistry transport model SILAM (backronym for System for Integrated modeLling of Atmospheric coMposition). The stratospheric balloon observations and retrievals from the limb-viewing **MIPAS** instrument operated on-board of the Envisat satellite in 2002-2012 are used as a validation for the simulated distribution.

With the results of these simulations we

- compare different methods of estimating the AoA and quantify inconsistencies in AoA and its trends arising from violations of the underlying assumptions behind each method
- analyze the causes of the discrepancies in the upper stratosphere between different methods of deriving the AoA
- provide a solid basis for further studies of stratospheric circulation with observations of various trace gases and for studies of climate effects of SF_6

The paper is organized as follows. Sec. 2 gives an overview of the modelling tools, and the modelling and observational data used for the study. Sec. 3 describes the developments made for ~~Silam~~ SILAM in order to perform the simulations: vertical eddy diffusivity parametrisation in ~~stratosphere and~~ the stratosphere and the lower mesosphere, and SF_6 destruction parametrization, as well as the modelling setup. The sensitivity tests and evaluation of the simulations against MIPAS satellite retrievals, and stratospheric-balloon measurements of SF_6 mixing ratios are given in Sec. 4. Sensitivity of AoA and its trends to the choice of the simulation setup and AoA proxy is studied in Sec. 5. The findings of the whole study are summarised in Sec. 7.

2 Methods and input data

2.1 SILAM model

SILAM (System for Integrated modeLling of Atmospheric coMposition) is an off-line chemical-transport model. SILAM features a mass-conservative and positive-definite advection scheme that makes the model suitable for long-term runs (Sofiev et al., 2015). The model can be run at a range of resolutions starting from a kilometer scale in limited-area or in global mode. The vertical structure of modelling domain consist of stacked layers starting from the surface. The layers can be defined either in z- or hybrid sigma-pressure coordinates. The model can be driven with a variety of NWP- (numerical weather prediction) or climate models.

In order to accurately model the AoA and needed tracers, the vertical diffusion part of the transport scheme of SILAM has been refined to account for gravitational separation. In addition, several tracers with ~~specific transformation procedures~~ corresponding transformation and transport routines have been implemented into the model. The ~~specific~~ model setup used for the present study is described in Sec. 3.5.

2.2 ECMWF ERA-interim reanalysis

The ERA-Interim reanalysis from the European Centre for Medium-range Weather Forecasts (ECMWF) had been used as a meteorological driver for our simulations. The data set has T255 spectral resolution and covers the whole atmosphere with 60 hybrid sigma-pressure levels (Dee et al., 2011), having the uppermost layer from ~~20~~ 0.2 to 0 ~~Pa~~ hPa with nominal pressure of ~~10 Pa~~0.2 hPa. The reanalysis uses a 12-h data assimilation cycle, and the forecasts are stored with a 3-hour time step. We used the fields retrieved form the ECMWF's MARS archive on a lat-lon grid 500x250 points with step of 0.72 degrees. The four forecast times (+3h, +6h, +9 h and +12h) were used from every assimilation cycle to obtain a continuous dataset with 3-hour time step. To drive the dispersion model, the data ~~for 1980-2015~~ on horizontal winds, temperature and humidity for 1980-2018 were used. The procedure for diagnosing the vertical transport is desctribed in Sec. 3.5.

The ERA-interim reanalysis has been used earlier for Lagrangian simulations of AoA (Diallo et al., 2012) and found to provide ages that agree with those inferred from in-situ observations in the lower stratosphere.

2.3 MIPAS observations of SF_6

To evaluate the results of SF_6 modelling we used the data from the MIPAS instrument operated on-board of Envisat satellite in 2002-2012. MIPAS was a limb-sounding Fourier transform spectrometer with a high spectral resolution measuring in the infrared. Due to its limb geometry, a good vertical resolution of the derived trace gas profiles and a high sensitivity to low-abundant species around the tangent point has been achieved. Along the orbit path, MIPAS measured a profile of atmospheric radiances about every $400\,\mathrm{km}$ with an altitude coverage, in its nominal mode, of about $6 - 70\,\mathrm{km}$~~altitude~~. The vertical sampling was $1.5\,\mathrm{km}$ in the lower part of the stratosphere (up to $32\,\mathrm{km}$) and $3\,\mathrm{km}$ above, with a vertical field of view covering $3\,\mathrm{km}$

at the tangent point. Over a day, about 1300 profiles along 14.4 orbits were measured, covering all latitudes up to the poles at sunlit and dark conditions. The vertical distributions of trace gases were derived from the radiance profiles by an inversion procedure, fitting simulated spectra to the measured ones while varying the atmospheric state parameters.

The retrieval of SF_6 is based on the spectral signature of this species in the vicinity of $10.55\,\mu m$ wavelength and is in principle described in Stiller et al. (2008, 2012); Haenel et al. (2015). In this study here, we use an updated version of SF_6 data (compared to the one described in Haenel et al. (2015)) called V5H/R_SF6_21/224/225; the absorption cross-section data on SF_6 and a new CFC-11 band in the vicinity of the SF_6 signature ~~provided by J. Harrison (pers. communication)~~ by Harrison (2018) has been used instead of the older cross section data by Varanasi et al. (1994). The updated version provides considerably higher SF_6 mixing ratios in the upper part of the stratosphere (above $30\,km$) than the versions before and is closer to independent reference data.

The retrieved profiles are sampled on an altitude grid spaced at $1\,km$, where as the actual resolution of the profiles is between 4 and $10\,km$ for altitudes below $30\,km$. The retrievals are supplemented with averaging kernels and error covariance matrices describing uncertainties due to ~~measurement noise~~random noise in the radiance measurements, called measurement noise error or target noise error or retrieval noise error in the following. This error component, which is normally in the order of 10% of the retrieved value, ~~and the correlations among the retrieved quantities. The error is uncorrelated between profiles, so, averaging makes it negligible in monthly zonal means~~is fully uncorrelated from profile to profile, and therefore virtually cancels out when averaging over a large number of profiles. In contrast, there exist systematic error components that are fully correlated between the profiles. Their assessment is difficult and depends on the knowledge about sources of systematic errors. Stiller et al. (2008) has assessed them to be in the order of 10% at 60 km, and 4% at 30 km. These error components have to be considered when comparisons of larger datasets (monthly or seasonal means) with other data are performed.

3 ~~Silam~~ SILAM developments

~~In this section we introduce a set of parametrizations implemented in Silam for this study.~~

3.1 ~~destruction~~

~~The vertical profiles of destruction rate~~Vertical profiles of diffusion coefficients. ~~(after Totterdill et al., 2015) and its approximation in range of 55-75 km, given by Eq. (1).~~

The destruction of atmospheric SF_6 occurs at altitudes ~~over~~ above 60 km (Totterdill et al., 2015) that fall within the topmost layer of the ERA-Interim. The exchange processes in the upper stratosphere and lower mesosphere have to be adequately parameterized together with the destruction process. In our simulations we have suppressed the transport with of SF_6 mean wind above the modelling domain top (0.1 hPa, 65 km) and parameterized the SF_6 loss due to the eddy and molecular diffusion towards the altitudes where destruction occurs. In this section we introduce the set of parametrizations that were implemented in SILAM for this study.

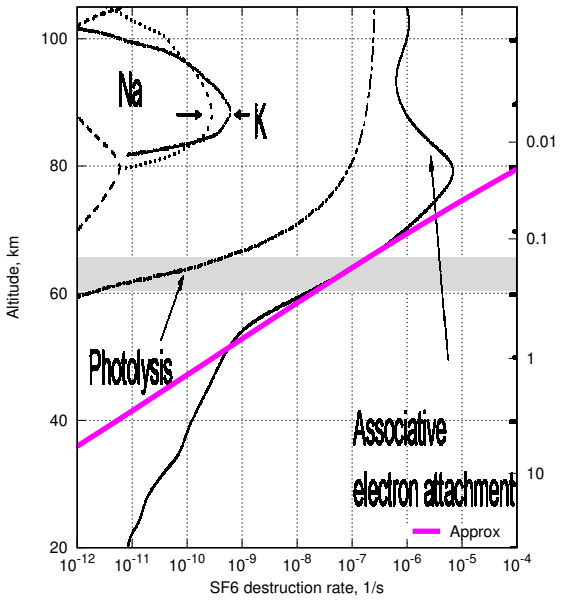

Figure 1. The vertical profiles of SF_6 destruction rate (after Totterdill et al., 2015) and its approximation in range of 55-75 km, given by Eq. (1).

3.1 SF_6 destruction

Estimates of AoA from the SF_6 tracer rely on the assumption of it being a passive tracer. SF_6 is indeed essentially stable ~~up to about 50 kmaltitudes. In the height~~ in the troposphere and stratosphere. IPCC (2013, Sec 8.2.3.5) mentions that photolysis in the stratosphere as the main mechanism of SF_6 loss, however without any reference to original studies. The statement is probably taken from Ravishankara et al. (1993). Reddmann et al. (2001) pointed associative electron attachment in the upper stratosphere and mesosphere as the main destruction mechanism for SF_6 below 80 km. The recent study of Totterdill et al. (2015) gives some 1-2 order of magnitude slower rates of electron attachment, however keeping it the dominant mechanism of the SF_6 destruction in the altitude range up to 100 km~~, the most pronounced destruction mechanism is associative electron attachment (Totterdill et al., 2015)~~. The highest destruction rate of ~~10^{-5} s^{-1}~~ 1×10^{-5} s^{-1} occurs at the altitude of 80 km (Fig. 1). An important feature of this profile is that the destruction rate becomes significant above the top of our modelling domain (~~10 Pa~~0.1 hPa, 65 km). The ERA-Interim meteorological fields have the uppermost level at ~~10 Pa~~ 0.1 hPa and do not resolve a vertical structure of the atmosphere above that level. In order to assess the loss of SF_6 due to destruction we have to parameterise the combined effect of ~~diffusion~~ transport of SF_6 ~~to the upper layers~~ transport through the 0.1 hPa and its destruction~~there~~. Then the ~~steady-state~~ resulting fluxes can be applied as the upper boundary condition ~~to~~ for our simulations.

As an approximation to the vertical profile of the destruction rate in an altitude range of 50–80 km we have fitted a corresponding part of the curve in Fig. 9a of Totterdill et al. (2015) with a power function of pressure (magenta line in Fig. 1):

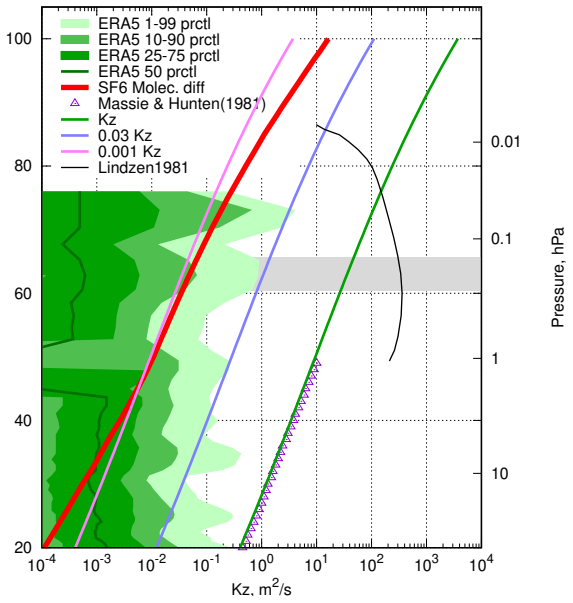

Figure 2. Vertical profiles of diffusion coefficients. The distribution of ERA5 profiles of the "mean turbulent diffusion coefficient for heat" parameter, molecular diffusivity for SF_6 in standard atmosphere, and three prescribed Kz profiles. The eddy diffusion profile due to breaking gravity waves (after Lindzen, 1981) is given for a reference.

$$\frac{1}{\tau} = 3 \cdot 10^{-8} s^{-1} 3 \times 10^{-8}\,\mathrm{s}^{-1} \left(\frac{20\,\mathrm{Pa}}{p} \frac{0.2\,\mathrm{hPa}}{p} \right)^3, \quad (1)$$

where τ is the lifetime of SF_6 at the altitude corresponding to pressure p.

3.2 Eddy diffusivity

Large variety of vertical profiles for eddy diffusivity in the stratosphere and lower mesosphere can be found in literature. In many studies in 1970-s – 1980-s the vertical profiles were derived from observed tracer concentrations neglecting the mean transport. Most studies suggested that the vertical eddy diffusion has a minimum of 0.2-0.5 m^2/s (Pisso and Legras, 2008) at 15-20 km agreeing quite well to the ones derived from radar measurements in the range of 15-20 km Wilson (2004). Above that altitude K_z was suggested to gradually increases by about 1.5 orders of magnitude at 50 km due to breaking gravity waves (Lindzen, 1981).

The theoretical estimates of the effective exchange coefficients considering the layered and patchy structure of stratospheric turbulence suggest 0.5–2.5 m^2/s for the upper troposphere and 0.015–0.02 m^2/s for the lower stratosphere (Osman et al., 2016), which is about an order of magnitude lower than the estimates above.

The values of eddy exchange coefficient at heights of 10-20km estimated from high-resolution balloon temperature measurements (Gavrilov et al., 2005) are ~ 0.01 m^2/s with no noticeable vertical variation. It is not clear, however, how representative the derived values are for UTLS in general. We could not find any reliable observations of vertical diffusion in a range of 30-50 km.

The parameterisation for vertical eddy diffusivity above the boundary layer used in SILAM has been adapted from the IFS model of the European Centre for Medium-range Weather Forecasts (ECMWF, 2015). However, in the upper troposphere the predicted eddy diffusivity is nearly zero. For numerical reasons a lower limit of 0.01 m^2/s is set for K_z in SILAM. Our sensitivity tests have shown that long-term simulations are ~~practically~~ insensitive to this limit as long as it is low enough (see results and discussion). The ~~modelled~~ K_z in the stratosphere is ~~practically always~~ routinely set to the limiting value with relatively rare peaks, mostly in UTLS. Such scheme essentially turns off turbulent diffusion in the stratosphere. Same is true for recent ERA5 reanalysis dataset (Copernicus Climate Change Service (C3S), 2017) that provides the values of K_z among other model-level fields: the eddy diffusion ~~practically always~~ routinely falls below the molecular diffusivity ~~limit~~ above 40 km (Fig. 2)~~, which is about two of orders of magnitude lower than the estimates referenced above~~.

As a reference for this study, we took a tabulated profile of Hunten (1975), as it was quoted by Massie and Hunten (1981). The original profile covers the range up to 50 km, and the extrapolation up to 80~~km matches well~~ km matches the theoretical estimates by (Lindzen, 1981) and by Allen et al. (1981). We approximate the profile as a function of pressure in the range of $100 - 0.01\,\mathrm{hPa}$ ($15 - 60\,\mathrm{km}$):

$$K_z(p) = 8\,\mathrm{m}^2/\mathrm{s}\left(\frac{100\,\mathrm{Pa}}{p}\frac{1\,\mathrm{hPa}}{p}\right)^{0.75}. \qquad (2)$$

The approximated profile was stitched with the default ~~Silam~~ SILAM profile with a gradual transition within an altitude range of $10 - 15\,\mathrm{km}$ to keep the tropospheric dispersion intact. This profile gives values of K_z is 3 – 6 orders of magnitude higher than ones ~~accepted in models~~ provided by ERA5 reanalysis (Fig. 2), and 1-2 orders of magnitude higher than more recent estimates (Legras et al., 2005).

In order to cover the ~~whole range of~~ range of vertical profiles of K_z ~~, along with~~ between ERA5 profiles and the reference one (2) we used two intermediate profiles ~~whose upper part was scaled~~ obtained by scaling the reference one with factors 0.03 and 0.001~~relative to the reference one~~. The three prescribed eddy-diffusivity profiles are hereinafter referred as “1Kz”, “0.03Kz”, and “0.001Kz” respectively. The dynamic eddy-diffusivity profile adopted from the ECMWF IFS model is referred to as “ECMWF Kz”. In all simulations the parameterization of K_z in the troposphere is the same, and linear transition from the SILAM K_z to the ~~tabulated~~ prescribed one occurs in the altitude range of $10 - 15\,\mathrm{km}$.

3.3 Molecular diffusivity and ~~gravity~~ gravitational separation

In tropospheric and stratospheric CTMs gaseous admixtures are transported as tracers, i.e. advection and turbulent mixing do not depend on a species properties, whereas the molecular diffusion is negligible. Models that cover the mesosphere, such as

WACCM (Smith et al., 2011), account for molecular diffusion explicitly. Since some of the K_z parametrizations above often result in values below the molecular diffusivity, the parametrization of molecular diffusion has been implemented in SILAM.

The molecular diffusivity of SF_6 in the air at temperature $T_0 = 300$ K and pressure $p_0 = 1000\,\mathrm{hPa}$, is $D_0 = 1 \times 10^{-5}\,\mathrm{m\,s^{-2}}$ (Marrero and Mason, 1972, Table 22). The diffusivity at a different temperature T and pressure p is given by:

$$D = D_0 \frac{p_0}{p} \left(\frac{T}{T_0} \right)^{3/2}, \tag{3}$$

see e.g. Cussler (1997). The vertical profile of molecular diffusivity in the US standard atmosphere (NOAA et al., 1976) is shown in (Fig. 2). Note that the value for the reference diffusivity of SF_6 used in this paper is about a half of the one used in simulations with WACCM by Kovács et al. (2017). The reason is that WACCM uses a universal parametrization (Smith et al., 2011, Eq. 7 there) for all compounds. That parametrization relies solely on molecular mass of a tracer and does not account for e.g. the molecule collision radius. The latter is about twice larger for SF_6 molecule than for most of stratospheric tracers. Thus, for this study we use the value from Marrero and Mason (1972), which results from fitting laboratory data for diffusion of SF_6 in the air.

The vertical diffusion transport velocity of admixture with number concentration $\tilde{n}$ and molecular mass $\tilde{\mu}$ in neutrally-stratified media is given by (Mange, 1957):

$$w = -D \left[\frac{1}{\tilde{\mu}} \frac{\partial \tilde{\mu}}{\partial z} + \left(\frac{\tilde{\mu}}{\mu} - 1 \right) \frac{\mu g}{kT} \right], \tag{4}$$

where μ is molecular masses of air, g – acceleration due to gravity, k is the Boltzmann constant, and T is temperature. With ideal gas law $p = nkT$, in which p is pressure, and n is number concentration, and static law $dp/dz = -g\rho$, where $\rho = \mu n$ is the air density, the equation (4) can be reformulated in terms of the admixture mixing ratio $\xi = \tilde{n}/n$ and pressure. Then the vertical gradient of the equilibrium mixing ratio will be:

$$\frac{\partial \xi}{\partial p} = \left(\frac{\tilde{\mu}}{\mu} - 1 \right) \frac{\xi}{p}. \tag{5}$$

It is non-zero for an admixture of a molecular mass different from one of the air. Integrating the gradient (5) over vertical, one can obtain that ~~the~~ equilibrium mixing ratios ~~of the admixture at two layers are proportional to the corresponding pressures taken to the power of $\tilde{\mu}/\mu - 1$.~~ ξ_1 and ξ_2 at two levels with corresponding pressures p_1 and p_2 are related as:

$$\frac{\xi_1}{\xi_2} = \left(\frac{p_1}{p_2} \right)^{\tilde{\mu}/\mu - 1}. \tag{6}$$

For heavy admixtures, such as SF_6 ($\tilde{\mu} = 0.146$ kg/mole) the equilibrium gradient of a mixing ratio is substantial. For example, the difference of equilibrium mixing ratio of SF_6 in the atmosphere between ~~10 and 20 Pa~~ 0.1 and 0.2 hPa is a factor of 16.

In most of the atmosphere, the effect of gravitational separation is insignificant due to the overwhelming effect of other mixing mechanisms, whereas in the upper stratosphere the molecular diffusivity may become significant. ~~Thus~~ Therefore, in the upper stratosphere heavy gases can no longer be considered as tracers and the molecular diffusion should be treated explicitly. The effect of gravitational separation of nitrogen and oxygen isotopes in the stratosphere has been observed ~~(Ishidoya et al., 2008)~~

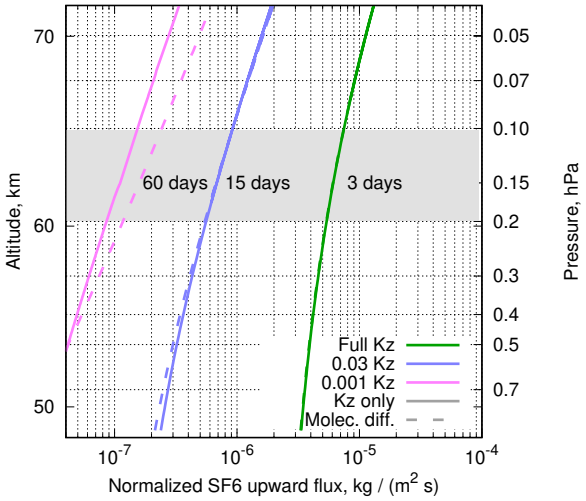

Figure 3. Vertical profiles of steady-state upward flux of SF_6 normalized with mass mixing ratio $F(p)/\xi(p)$, for eddy diffusivity and lifetime profiles given by (2) and (1). The upper model layer of ~~Silam~~ SILAM and effective lifetimes of SF_6 there due to the destruction in the mesosphere for different ~~K~~ Kz profiles are given.

(Ishidoya et al., 2008, 2013; Sugawara et al., 2018), however for isotopes the ratio of masses is relatively small, so the observed differences were also small (up to 10^{-5}). For SF_6 the molecular mass difference is much larger.

In order to enable the gravitational separation in SILAM we have introduced a molecular diffusion mechanism~~that~~, which can be enabled along with the turbulent ~~vertical~~ diffusion scheme. The exchange coefficients due to molecular diffusion between the model layers are pre-calculated according to Eq. (4) ~~discretised~~ discretized for the given layer structure for each species according to its diffusivity and molar mass. The US standard atmosphere (NOAA et al., 1976) was assumed for vertical profiles of temperature and air density during pre-calculation of the exchange coefficients. The exchange has been applied throughout the domain at every model time step with a simple explicit scheme.

3.4 Parametrization for destruction of SF_6 in the mesosphere

As it has been mentioned above, the topmost level of the ERA-Interim meteorological data set is located at ~~10 Pa~~0.1 hPa, which is below the layer where the destruction of SF_6 occurs. Therefore we have to put a boundary condition to our simulations to account for the upward flux of SF_6 through the upper boundary of the simulation domain. For that we assume that SF_6 distribution above the computational domain is in equilibrium with destruction and vertical flux.

Assuming the profiles for $K_z(p)$ and the SF_6 lifetime $\tau(p)$ are given by (2) and (1), one can obtain a steady-state distribution of mass-mixing ratio ξ of SF_6 due to destruction in the mesosphere at any point where both (2) and (1) are valid and vertical advection is negligible. ~~This requires~~ The latter assumption implies that the diffusive vertical flux overwhelms the advective one. The validity and implications of neglecting the regular vertical transport are discussed below. The steady-state profile of ξ

can be obtained from a solution of a steady-state diffusion equation with a sink:

$$\frac{\partial \xi}{\partial t} = g^2 \frac{\partial}{\partial p}\left(\rho^2 K_z(p)\frac{\partial \xi}{\partial p} F\right) - \frac{\xi}{\tau(p)} = 0, \tag{7}$$

where $\rho(p)$ is air density, and g is acceleration due to gravity. ~~Solving the Eq. (7) one can express the steady-state~~ , and the upward flux of SF_6 ~~normalized with the mass mixing ratio at each pressure $\tilde{F}(p) = F(p)/\xi(p)$ as a function of p.~~ is given by

$$F(p) = g\rho^2 K_z(p)\frac{\partial \xi}{\partial p} \tag{8}$$

The above equation was solved numerically ~~with a boundary conditions of~~ as a boundary value problem with unit mixing ratio at a height of ~~100 Pa~~ 1 hPa and vanishing flux $F(p)$ at $p = 0$ ~~. Indeed for~~ for the set of Kz profiles. The shooting method was used together with bisection to get the steady-state profiles of $\xi(p)$ and $F(p)$, corresponding to $\xi(1\,\mathrm{hPa}) = 1$. For all considered cases the flux $F(p)$ decreased by several orders of magnitude already at the level of a few Pa. ~~The resulting $\tilde{F}(p)$ for four~~ , i.e. below the maximum of the depletion profile of Totterdill et al. (2015), indicating that particular shape of $\tau(p)$ above that level does not influence the fluxes at the domain top (0.1 hPa). The steady-state upward flux of SF_6 $F(p)$ normalized with corresponding mixing ratio at each pressure $F(p)/\xi(p)$, for the three test profiles of K_z ~~are~~ is shown in Fig. 3 with solid lines.

The ~~effect of~~ gravitational separation can be accounted for by introducing into the vertical flux Eq. (~~7~~8) a term responsible for molecular diffusion and its equilibrium state (5):

$$\frac{\partial \xi}{\partial t} F(p) = g^2 \frac{\partial}{\partial p}\rho^2 K_z(p)\frac{\partial \xi}{\partial p} + g\rho^2 D(p)\left(\frac{\partial \xi}{\partial p} - \frac{\tilde{\mu}-\mu}{\mu}\frac{\xi}{p}\right) - \frac{\xi}{\tau(p)} = 0. \tag{9}$$

The profiles of ~~$\tilde{F}(p)$ resulting form this equation for~~ $F(p)/\xi(p)$ resulting from this term $F(p)$ in the equation (7 are given in Fig. 3 with dashed lines. The magnitude of $F(p)/\xi(p)$ gives an equivalent regular vertical air-mass flux that would result in the same vertical flux of SF_6 if it were passive and non-diffusive. The equivalent regular vertical velocity ω_{eq} (in units of the Lagrangian tendency of a parcel pressure due to vertical advection) can be expressed as:

$$\omega_{eq} = -gF(p)/\xi(p). \tag{10}$$

Accounting for molecular diffusion may either enhance or reduce the upward flux of SF_6 in the model. Along with setting the equilibrium state ~~when~~ with the bulk of a heavy admixture ~~is~~ being in the lower layers, molecular diffusion provides additional means for transport to the upper layers where the destruction occurs. For very low eddy diffusivities, the molecular diffusion is a sole mechanism of upward transport of SF_6 towards depletion layers. For higher eddy diffusivity the effect of molecular diffusion and gravitational separation becomes negligible.

For a model consisting of stacked well-mixed finite layers, the loss of SF_6 from the ~~uppermost~~ topmost layer due to the steady upward flux would be proportional to the SF_6 mixing ratio in the layer. This loss of mass is equivalent to a linear decay

of SF_6 in the layer at a rate ~~$\tau^{-1} = g\tilde{F}(p)/\Delta p$,~~

$$\tau^{-1} = g\frac{F(p)}{\xi(p)\Delta p}, \tag{11}$$

where Δp is a pressure drop in the layer.

For the upper layer of our simulations ~~, the layer between 10 and 20 Pa (~~(between 0.1 hPa and 0.2 hPa, grey rectangle in Fig. 3), and $K_z(p)$ given with Eq. (2), the ~~corresponding~~ SF_6 lifetime τ ~~in the layer~~ due to turbulent diffusion is about 3 days. After scaling the $K_z(p)$ profile with factors of ~~0.1, 0.01~~0.03, and 0.001 one gets the lifetimes of ~~8, 30,~~ 15 and 60 days respectively. ~~Note that due to~~ Noteworthy, the molecular diffusion ~~,~~ sets the upper limit to the SF_6 lifetime in the topmost model layer: it can not be longer than 60 days for the 0.1 - 0.2 hPa layer. Close to this regime, the system becomes insensitive to the ~~exact profile of the eddy diffusivity. In particular, for the considered layerit can not be longer than 60 days~~actual profile and values of the turbulent diffusion coefficient. The loss of SF_6 through the domain top was implemented as a linear decay of SF_6 in the topmost model layer, at a rate corresponding to the $K_z(p)$ profile used in each simulation.

3.5 Simulation setup

The simulations of atmospheric transport were performed with the SILAM model for 1980-2018 years on a 1.44x1.44 degree global grid with 60 hybrid sigma-pressure layers starting from surface, with the uppermost layer between pressures of ~~20 and 10 Pa~~0.1 and 0.2 hPa. The model time step of 15 minutes was ~~been~~ used and the output of daily mean concentrations of tracers together with air density was arranged.

The simulations were driven with ERA-interim meteorology at 0.72-degree resolution, so the meteorological input for both cell-interface for winds, and cell mid-points for other parameters (surface pressure, temperature and humidity) was available without further interpolation. The gridded ERA-interim fields are, however, a result of reprojection of the original meteorological fields from spherical harmonics. Moreover, differences in the representation of model vertical structure between IFS and SILAM make a vertical reprojection necessary. These reprojections together with a limited precision of the gridded fields and inevitable small differences in physical parametrizations between IFS and SILAM result in inconsistency between surface-pressure tendencies and vertically-integrated air-mass fluxes calculated from the meteorological fields in SILAM. Such inconsistencies cause spurious variations in wind-field divergence that on long-term run result in accumulation of errors in tracer mixing ratios, and consequently, in the simulated AoA. Therefore, horizontal wind fields were adjusted by distributing the residuals of pressure tendency and vertically-integrated horizontal air-mass fluxes as a correction to the horizontal winds following the procedure suggested by Heimann and Keeling (1989). The correction is ~~normally~~ of the order of centimeters per second, which is comparable to the precision of the input wind fields. The vertical wind component was then re-diagnosed from a divergence of horizontal air-mass fluxes for individual SILAM layers as described in Sofiev et al. (2015).

SILAM performs 3D transport by means of a dimension split: transport along each dimension is performed separately as 1D transport. To minimize the inconsistency between the tracer transport and air-mass fluxes, caused by the dimension split at finite time step, the splitting sequence has been inverted at each time step to reduce the accumulation of errors. The residual inconsistency was resolved by using a separate ~~"ones"~~ unity tracer, which was initialized to the constant mass mixing ratio of 1

at the beginning of a simulation. If advection was perfect, the concentration of ~~"ones"~~ unity would be equivalent to air density (mixing ratio would stay equal to 1). The mixing ~~rations~~ ratios of simulated tracers were then evaluated as a ratio of a tracer mass in a cell to the mass of ~~"ones"~~unity.

In order to assess the effects of gravitational separation and destruction on the atmospheric distribution of SF_6, we have used four tracers: SF_6 as a passive tracer "sf6pass", SF_6 with gravitational separation but no destruction "sf6nochem" (no chemistry), SF_6 with destruction but no gravitational separation "sf6nograv", and SF_6 with both gravitational separation and destruction in the upper model level "sf6".

All SF_6 tracers had the same emission according to the SF_6 emission inventory (Rigby et al., 2010). The inventory covers 1970-2008, and was extrapolated with a linearly growing trend of ~~0.294 Gg/y~~ 0.294 Gg/y/y until July 2016. The last 2.5 years were run without SF_6 emissions to evaluate its destruction rate. Note, that the emission extrapolation gives for 2016 9.4 Gg/y, which is somewhat higher than later estimate 8.8 Gg/y (Engel et al., 2018).

Besides the four SF_6 tracers we have used a "passive" tracer emitted uniformly at the surface at constant rate during the whole simulation time and an "ideal age" tracer. The "ideal age" tracer is defined as a tracer whose mixing ratio ξ_{ia} obeys continuity equation (Waugh and Hall, 2002):

$$\frac{\partial \xi_{ia}}{\partial t} + \mathcal{L}(\xi_{ia}) = 1, \tag{12}$$

(where $\mathcal{L}$ is an advection-diffusion operator), and boundary condition $\xi_{ia} = 0$ at the surface. The "ideal age" tracer is transported as a regular gaseous tracer, and to maintain consistency with other tracer mixing ratios, the ideal age is updated at every model time step Δt using the ~~"ones" tracer:~~ unity tracer:

$$M_{ia} \mapsto \begin{cases} 0, & \text{at lowest layer,} \\ M_{ia} + M_{\text{unity}} \Delta t, & \text{otherwise,} \end{cases} \tag{13}$$

where M_{ia} and ~~M_{ones}~~ M_{unity} are masses of the "ideal age" tracer and of ~~"ones"~~ the unity tracer in a grid cell. The mixing ratio of the "ideal age" tracer is a direct measure of the mean age of air in a cell, so the tracer is a direct Eulerian ~~analogy~~ analog of the time-tagged Lagrangian particles with clock reset at the surface. Note that the AoA derived from the "ideal age" tracer and AoA from a passive tracer with a linearly-growing near-surface mixing ratio are equivalent (Waugh and Hall, 2002), and implementation of both provides a redundancy needed to ensure self-consistency of our results.

A set of the simulations was performed with four settings for the eddy diffusivity profile within the model domain, described in Sec. 3.2 and corresponding destruction rates of "sf6" and "sf6nograv" tracers in the uppermost model layer. All runs were initialized with the mixing ratios from the final state of a special initialization run~~performed with "0.001~~. The initialization simulation with "0.1Kz" eddy diffusivity ~~. The initialization simulation~~ was started from 1970 with zero fields for all tracers, except for ~~"ones"~~ unity tracer that was set to unity mixing ratio. The simulation was run with ~~1970-1979~~ 1970-1989 emissions for SF_6 species from the same inventory as for the main runs (Rigby et al., 2010), and driven ~~by~~ with twice repeated ERA-Interim meteorological fields for 1980-1989. The mixing ratios of all SF_6 tracers at the end of the initialization run were scaled to match the total SF_6 burden of 20.17 Gg in 1980 (Levin et al., 2010).

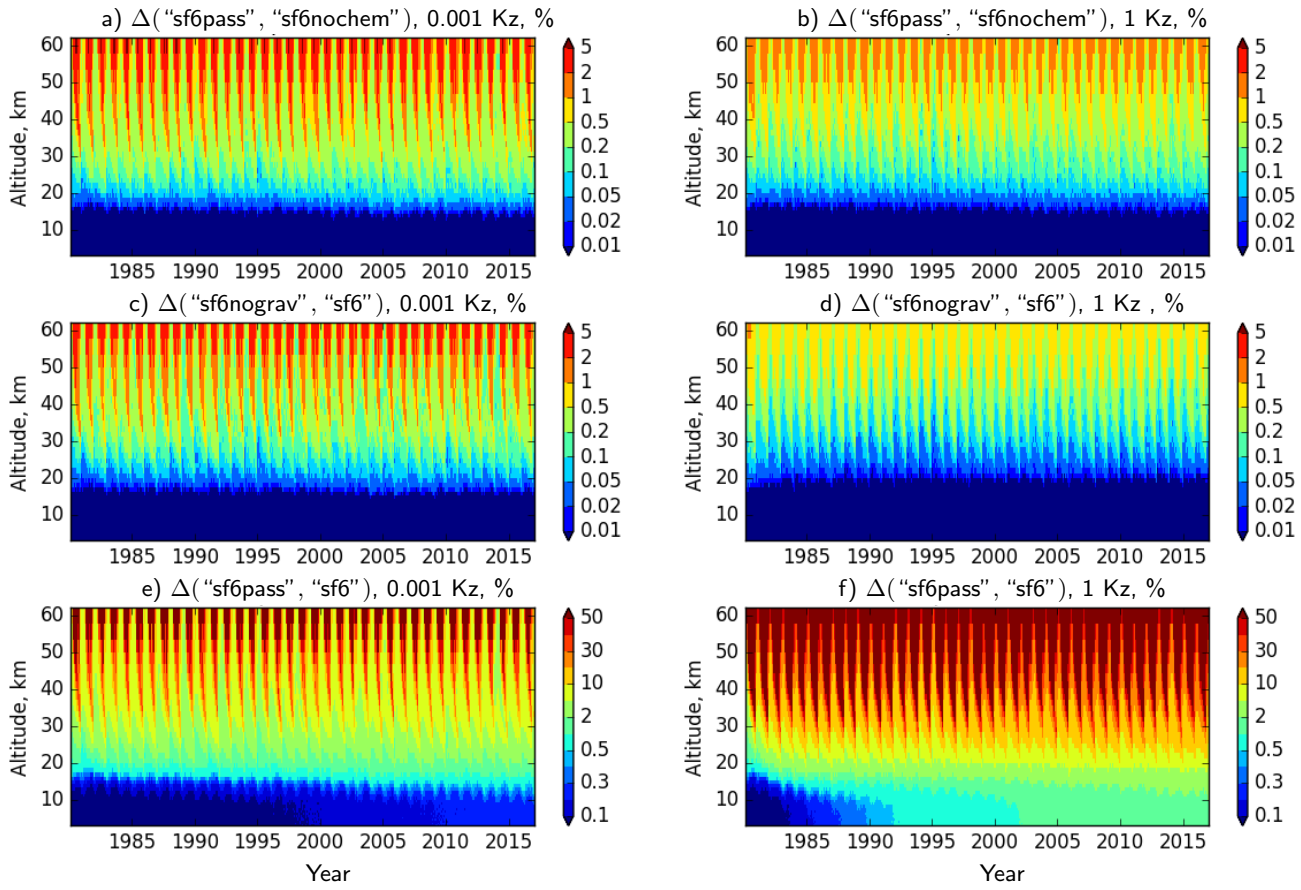

Figure 4. The relative reduction of SF_6 content (in %) at 70-85S due to gravitational separation with (a, b) and without (c, d) depletion, and due to combined effect of depletion and separation (e, f) at two extreme Kz cases. Note different color scales for e) and f).

4 Sensitivity and validation of SF_6 simulations

4.1 Gravitational separation and mesospheric depletion

To evaluate the relative importance of gravitational separation and mesospheric depletion and their effect on the SF_6 concentrations we have compared the simulations for various SF_6 tracers and evaluated the relative reduction of SF_6 content in the stratosphere due to these processes. As a conservative estimate of the reduction, we evaluated the relative differences between the tracers in the latitude belt of 70-85S, since both processes have the most pronounced effect in southern polar vortex, where the ~~downdraught~~ downwelling of Brewer-Dobson circulation is the strongest.

Hereafter we quantify the effect of a relative difference between atmospheric contents of two SF_6 tracers "X" and "Y" defined as:

$$\Delta(\text{"X"},\text{"Y"}) = 2\frac{\xi_X - \xi_Y}{\xi_X + \xi_Y} \cdot 100\% \quad (14)$$

The relative differences for the SF_6 tracers in the Southern polar region (70-85S) simulated with two extreme models for K_z is given in Fig. 4 as a function of time and altitude. Noteworthy, every 5% of decrease of SF_6 with respect to its passive counterpart correspond to about one year of a positive bias in AoA derived ~~form~~ from SF_6 mixing ratios.

The reduction of SF_6 content due to gravitational separation if the mesospheric depletion is disabled is given by the relative difference of "sf6nochem" and "sf6pass" (Fig. 4ab). Expectedly, the effect of gravitational separation is most pronounced for the case of low eddy diffusivity ("0.001 Kz"), and the reduction of SF_6 in the altitude range of 30–50 km reaches 2 – 5 %. In the case of strong mixing, the effect of separation is about 1 %.

The reduction of SF_6 content due to gravitational separation in presence of stratospheric depletion given by the relative difference of "sf6nograv" and "sf6" tracers. The effect of the separation for low K_z is very similar between depletion and no-depletion case (Fig. 4c vs. Fig. 4a). Depletion reduces the effect of the gravitational separation for high K_z (Fig. 4b vs Fig. 4d). Regardless depletion, stronger K_z reduces the effect of the gravitational separation, however the latter is still non-negligible if precisions of order of a month for AoA are required.

.

The combined effect of depletion and gravitational separation is seen in the relative difference of "sf6pass" and "sf6" tracers (Fig. 4e and 4f). For both K_z cases the effect of depletion is stronger than diffusive separation by more than ~~an~~ one order of magnitude~~stronger than one of gravity separation. Regardless the used~~ . Regardless of the K_z profiles used, the reduction exceeds 50 %, which roughly corresponds to 10 years of an offset in the apparent AoA. ~~The~~

In all cases the reduction of the SF_6 content has strong annual cycle associated with the cycle of downwelling in winter and upwelling in summer. Besides that reduction has a noticeable inter-annual variability that poses substantial difficulties on applying a consistent correction to the apparent AoA. Contrary to the former two comparisons, ~~stronger~~ strong eddy mixing leads to ~~stronger~~ strong reduction of SF_6 since it intensifies the transport to the depletion layers, and thus enhances the depletion rate.

~~Since the~~ The simulations for different K_z have been initialized with the same state ~~matching the total amount of , the simulations~~ obtained from a separate spin-up simulation with "0.01 Kz"~~showed~~ , which was scaled to match total burden of SF_6 in 1980. Thus a relaxation of the SF_6 vertical distribution during the first few years of the simulations is clearly seen in Fig. 4. For "1 Kz" case (4f) the gradual increase of the difference between SF_6 and its passive version in the troposphere can be seen. The rate of this increase is about 0.5% per 39 years of simulations. This rate should not be confused with the depletion rate of SF_6 in the atmosphere since the difference is a combined effect of depletion and growth of emission rate, despite the latter is exactly the same for both tracers. –

The above comparison indicates that the depletion has the stronger effect on the distribution of the SF_6 mixing ratio in the upper stratosphere than gravitational separation and molecular diffusion. However, the important role of the molecular diffusion in the model is that it maintains the upward flux towards the mesosphere in the simulations even if the eddy diffusivity ceases.

Further in this paper only the "sf6pass" and "sf6' tracers will be used.

4.2 ~~Lifetime of in the atmosphere~~

~~The time series of mean mixing ratio of in the atmosphere simulated with emissions stopped in July 2016. The total burden by Levin et al. (2010) and by Rigby et al. (2010) are shown for comparison.~~

~~Tracer/ removal rate, lifetime, Kz scheme 10^3 mol/year years passive, any Kz 0 ∞ , ECMWF Kz 440 2900 , 0.001 Kz 480 2600 , 0.01 Kz 760 1700 , 0.03 Kz 800 1540 , 0.1 Kz 960 1300 , 1 Kz2160 590 destruction rate after stopping emissions. Mid-2011 atmospheric burden of of $1.27 \cdot 10^9$ moles is used as reference for the lifetime estimate~~

~~In order to estimate the atmospheric lifetime of we turned off the emission of all simulated tracers in July 2016 and let the model run until the end of 2018 without emissions (Fig. 9). The decrease of the simulated burden after the emission stop can be used to estimate the removal rate from the atmosphere.~~

~~Time series of the total burden of in the atmosphere in the simulations are given in Fig. 9. For easier comparison to observed mixing ratios the burden has been normalised with $1.78 \cdot 10^{20}$ moles – the total amount of air in the atmosphere – to get the mean mixing ratio. The tabulated values for the atmospheric burden of from Levin et al. (2010) and Rigby et al. (2010) are given for comparison. Since the removal of from the atmosphere is mostly controlled by the transport towards the depletion layer, the vertical exchange is a key controlling factor. In all simulated cases, the removal of from the atmosphere is very slow, so the relative difference between the cases is small.~~

~~The decrease of the atmospheric content after the emission stop, is given at the zoom panel of Fig. 9. As expected, after July 2016 the content of passive stays constant, while depleting start to fall down at a rate that depends on the transport properties of the stratosphere in the simulations, with faster removal for stronger eddy diffusivity. The removal rate is driven by the content in the upper stratosphere, which is not in equilibrium with total atmospheric content. A typical delay between mixing ratio in the troposphere, where most of resides, and the upper stratosphere, from where escapes further to the depletion layers, is about 5-6 years. Hence, to estimate the lifetimes we used the total amount of atmospheric 5 years before the emission stop, i.e. 1.23×10^9 mol, which corresponds to mean mixing ratio of about 7 pmol/mol. Dividing the destruction rate with the reference amount one gets the range of corresponding simulated life times in the atmosphere: 600 to 2900 years. Despite the range of assumed diffusivities is three orders of magnitude, the decay rate of varies only within a factor of five (Table 1).~~

~~The range of the life times meets the ranges suggested by earlier studies. It is in a good agreement with results of Kovács et al. (2017) , who obtained 1120 – 1475 years, and within the range of 800 – 3200 years, that one can find from model studies (Ravishankara et al., 1993; , and 580–1400 years estimated from observational data (Ray et al., 2017).~~

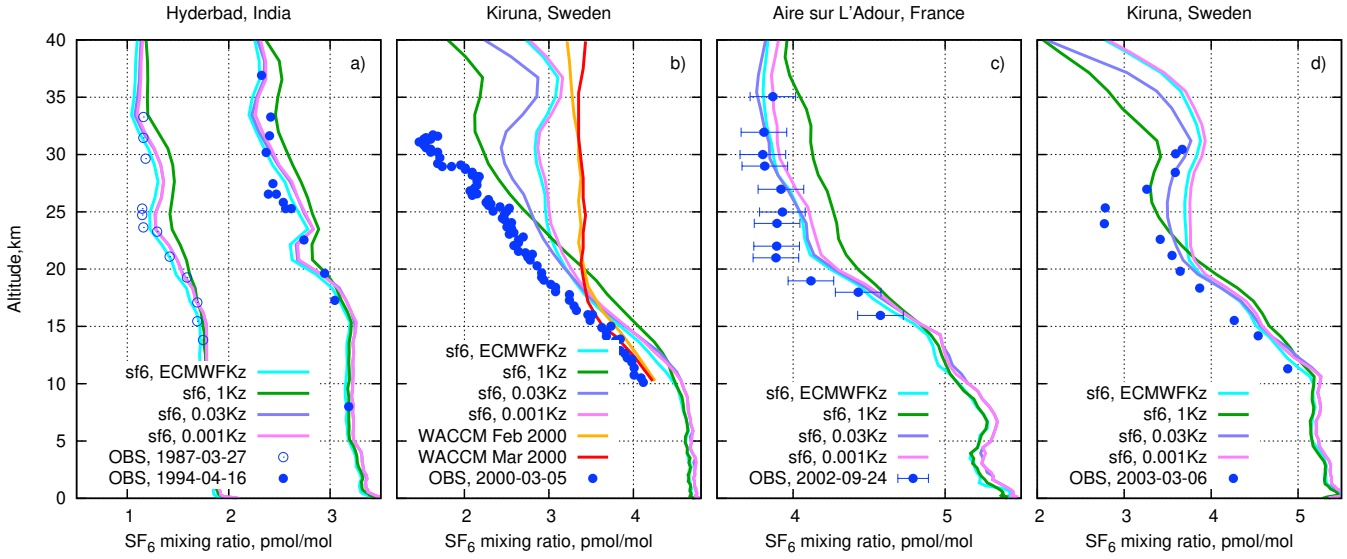

Figure 5. Observed SF_6 balloon profiles and corresponding daily-mean SILAM profiles for the date of observations. The observational data obtained from Patra et al. (1997), Ray et al. (2017), Ray et al. (2014), and Engel et al. (2006) for panels a–d correspondingly. The model profiles from WACCM model are from Ray et al. (2017).

4.2 Evaluation against balloon profiles

The tropospheric concentrations of SF_6 in our simulations have been ~~practically insensitive to the way and rate of~~ insensitive to SF_6 destruction or to the choice of the eddy diffusivity profile in the stratosphere. The difference in the modelled profiles can however be seen above the tropopause. For comparison we took the simulations with prescribed eddy diffusivity in stratosphere (1Kz, 0.03Kz, and 0.001Kz, see Sec. 3.2), and with dynamic eddy diffusivity "ECMWF Kz". The simulations were matched with stratospheric balloon observations ~~we have found in a literature~~ (Fig. 5) published by Patra et al. (1997); Engel et al. (2006); Ray et al. .

Two balloon profiles observed at Hyderbad (17.5N,78.6E) in 1987 and 1994 by Patra et al. (1997) indicate an increase of SF_6 content during the time between the soundings (Fig. 5a). Both profiles have a clear transition layer from tropopause at ~ 17 km to undisturbed upper stratosphere above ~ 25 km. The simulated profiles agree quite well to the observed profiles, except for the most diffusive case that gave notably smoother profiles and somewhat overstated SF_6 mixing ratios due to too strong ~~exchange~~ upward transport by the diffusion through the tropopause and in the lower stratosphere.

The profile in Fig. 5b has been obtained from Kiruna (68N, 21E) in early spring 2000 during the SAGE III Ozone Loss and Validation Experiment, SOLVE, (Ray et al., 2002) with the Lightweight Airborne Chromatograph (Moore et al., 2003). The profile is affected by the polar vortex and clearly indicates a strong reduction of SF_6 with height with a pronounced local minimum at 32 km. The corresponding SILAM profiles tend to overestimate the SF_6 vmr. The SF_6 profiles for "ECMWF

Kz" ~~profile practically coincides to~~ and "0.001Kz" match each other, since vertical mixing is negligible in both cases. The most diffusive profile "1Kz" has the strongest depletion in the upper part, but the largest deviation from the observations below 20 km. The intermediate-diffusion profile ("0.03Kz") is almost as close to observations as the non-diffusive profile. Moreover, the "0.03Kz" profile has a minimum at the same altitude as the observed one, albeit the modelled minimum is substantially less deep.

For comparison, Fig. 5b also contains monthly-mean profiles from the WACCM simulations of ~~Ray et al. (2014)~~ Ray et al. (2017) along with the observation data. The WACCM profiles match very well the observations below 17 km, but turn nearly constant above, thus under-representing the depletion of SF_6 inside the polar vortex. Monthly-mean SILAM profiles (not shown) were much closer to plotted daily profiles than to monthly WACCM ones. Note, that the version of WACCM, used for the simulations did not include the electron attachment mechanism.

For the mid-latitude profile in Fig. 5c from Aire-sur-l'Adour, France (43.7N,0.3W), all SILAM profiles except for "1Kz" ~~practically~~ fall within the observational error bars provided together with the data by Ray et al. (2017). Similar to the Kiruna case in Fig. 5b, the SILAM profiles are much smoother than the observed ones and are unable to reproduce the sharp transition at 20 km.

Another profile from within the polar vortex (Fig. 5d) was observed at the same Kiruna site as the one in Fig. 5b, but three years later. The observed profile also has a minimum that is much deeper than in the modelled profiles. Similar to the case in Fig. 5b, the "0.03Kz" profile is the only one that has a pronounced minimum at the same altitude as the observed one. The minimum is a result of the spring breakdown of the polar vortex, when a regular down draught ceases, and atmospheric layers decouple from each other. The reduced depth of the modelled minimum is probably caused by insufficient decoupling of the layers in the driving meteorology.

In all above cases, the "1Kz" profile is clearly far too diffusive: in non-polar cases and is an outlier that is ~~furthermost~~ furthest from the observations. ~~The~~ , whereas for Kiruna cases it overstates the lower part of the profiles and smears the vertical structure of the profiles further away form the tropopause. The SF_6 profiles simulated with "ECMWF Kz" ~~profiles practically coincide to~~ and "0.001Kz" match each other in all simulations, since vertical mixing is negligible in both cases. The SF_6 resulting from "0.03Kz" ~~profiles~~ case appear to be most realistic out of the four considered simulations: they are close to observed ones and have local minima at right altitudes for both Kiruna profiles.

4.3 Evaluation of SF_6 against MIPAS data

The MIPAS observations provide the richest observational dataset for stratospheric SF_6. However, each individual observation has a substantial retrieval noise error, which is noticeably larger than the difference between observation and any of the SILAM simulations. The largest diversity of the modelled SF_6 profiles was observed in polar regions, therefore below we show the mean profiles for each season in southern and northern polar areas. Besides that, we consider statistics of the model performance against MIPAS measurements in lower and upper stratosphere separately. For simplicity, we do not show the statistics for the "ECMWF Kz" runs, since it is very similar to one for "0.001Kz".

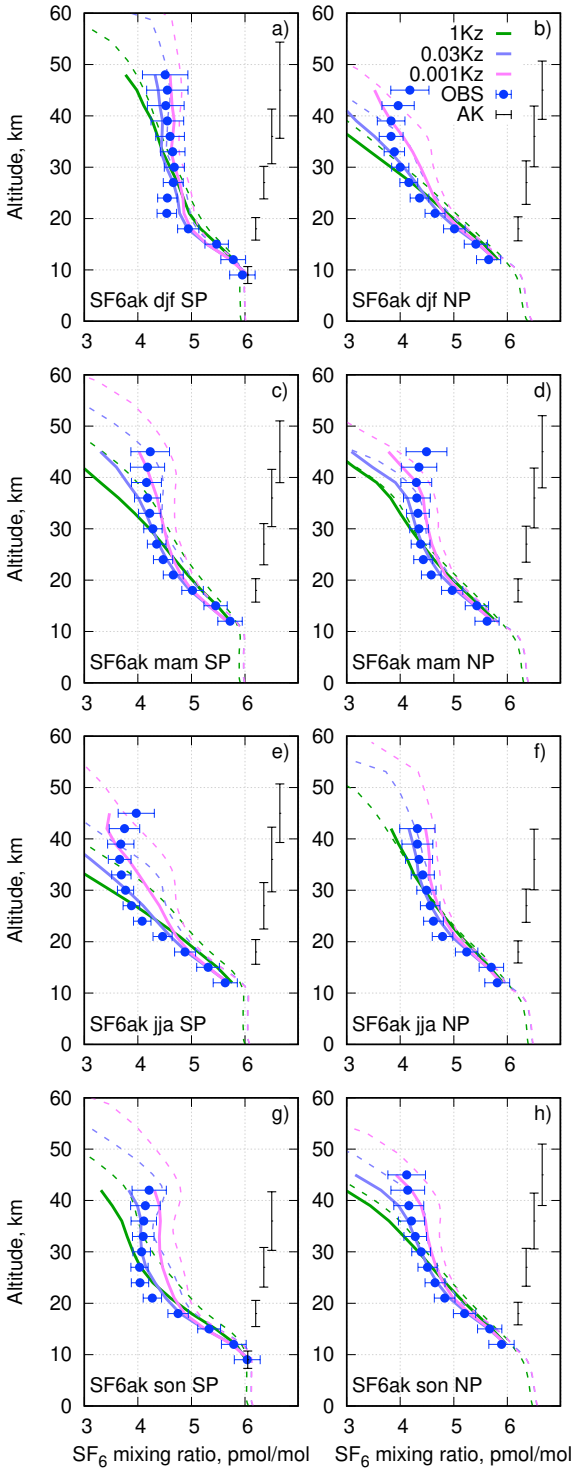

Figure 6. Seasonal mean collocated SILAM SF_6 and MIPAS profiles for 2007, for southern and northern polar regions. Typical ranges covering 75% of averaging kernel are given with error bars at the right-hand side of each panel. The horizontal error bars indicate systematic uncertainties of the observations that are fully correlated among profiles and do not cancel out when averaging over a large number of measurements.

For the comparison, the daily mean model profiles ~~have been~~ were collocated to the observed ones in space and time, and then, an averaging kernel of the corresponding MIPAS profile was applied to the SILAM profile. For the comparison we took only the data points with all the following criteria met:

- MIPAS visibility flag equals 1
- MIPAS Averaging kernel diagonal elements exceed ~~0.01~~ 0.03
- MIPAS retrieval vertical resolution, i.e. full-width at half-maximum of the row of the averaging kernel, is better than $20\,\mathrm{km}$
- MIPAS volume mixing ratio noise error of SF_6 is less than $3\,\mathrm{pmol/mol}$

The mean seasonal profiles of the SF_6 mixing ratio for southern and northern polar regions derived from the MIPAS observations and SILAM simulations for 2007 are given in Fig. 6. In order to facilitate the comparison of our evaluation with earlier study by Kovács et al. (2017) we have chosen the same year and same layout of the panels as Fig. 3 there. The main differences between Kovács et al. (2017) and current evaluation are:

- We used averages of collocated model profiles (bold lines). The non-collocated seasonal- and area-mean model profiles are given with thin dashed lines for comparison.
- we use a newer version of MIPAS SF_6 data with considerably larger values (up to 0.6 pptv) in the upper stratosphere, compared to the version that was used by Kovács et al. (2017).
- ~~We do not put~~ The horizontal error bars for the observed data ~~, since the statistical uncertainty of the averaged values in the scale of the plots is smaller than a data point size. In Kovács et al. (2017) the bars are standard deviations of the~~ indicate the systematic error component that is fully correlated among the profiles and does not cancel out by averaging, or, in other words, the estimate of a possible bias, as analysed by Stiller et al. (2008). These errors are in the order of 4% (below 30 km) up to 10% (at 60 km). The contribution of retrieval noise error is essentially negligible due to averaging. The error bars shown by Kovács et al. (2017) are noticeably larger, probably indicating that they are for individual observed values, rather than uncertainties of the mean.
- We use 3-km vertical bins for the profiles to make the points in MIPAS profiles distinguishable
- We also plot the vertical extent of the averaging kernels corresponding to their half-width.

First of all, note a substantial difference between collocated and non-collocated model profiles. The difference is caused by uneven sampling of the atmosphere by the satellite both in space and time. In particular, MIPAS, being a polar-orbiting instrument, makes more profiles per unit area closer to ~~a~~ the pole than further away. The difference gets somewhat reduced if one uses equal weights for all model grid cells instead of area-weighted averaging, especially for wide latitude belts. The major difference comes probably from the inability of MIPAS to retrieve SF_6 profiles in presence of polar stratospheric clouds that

clutter lower layers of the stratosphere and make the sampling of polar regions quite uneven both in time and in vertical. This hypothesis agrees with fact that the difference is most pronounced for the winter pole, especially for the south pole in JJA, and ~~practically negligible~~ almost invisible at a summer pole.

The comparison in Fig. 6 shows that the profiles from the SILAM simulations agree quite well to the observations in the altitude range below $20 - 25\,\mathrm{km}$, with the most diffusive "1Kz" slightly ~~overstating~~ overestimating the SF_6 mixing ratios. In the range above $25\,\mathrm{km}$, the '1Kz" profiles indicate too fast decrease of SF_6 with altitude. The "0.03Kz" profiles give the best results up to $\sim 40\,\mathrm{km}$, except for south pole in JJA and North pole in DJF.

An interesting feature of the winter-pole MIPAS profiles is an increase of the SF_6 mixing ratio above $40\,\mathrm{km}$. This increase might have been caused by issues with retrievals, as the systematic errors of the retrievals increase with altitude. Note, however, that non-monotonous profiles can occur due to the mean atmospheric dynamics (see the non-collocated 0.001Kz profile in Fig. 6g).

None of the model setups is capable of reproducing adequately the observations above 40 km. Wintertime poles also pose a problem to the model. The disagreement indicates a deficiency in the model representation of air flows in the upper part of the domain caused by insufficient vertical resolution of ERA-Interim in the upper stratosphere and lower mesosphere, and lack of pole-to-pole circulation. This discrepancy is in line with the comparisons in Fig. 5 for polar regions. The model tends to overstate the SF_6 content in the lower part of a polar vortex, and understate it above $40\,\mathrm{km}$.

As a more extensive verification of the SILAM simulations we computed statistical scores of the simulated SF_6 mixing ratios for each month of the MIPAS mission. The statistics were computed separately for the altitude range of $10 - 35\,\mathrm{km}$ (Fig. 7) and $30 - 60\,\mathrm{km}$ (Fig. 8). As the difference in ~~statistical scores of~~ the statistical scores between the three selected simulations shown in the two figures is quite minor, in addition to the aforementioned selection criteria for MIPAS data, we have selected only observations with the retrieval target noise error below $1\,\mathrm{pmol\,mol^{-1}}$.

–

The root-mean square error of is mostly controlled by the bias, and does not allow for clear distinction between the simulated cases. In order to disentangle the effect of bias, we have calculated the standard deviation of model-measurement difference (STD), absolute bias, and normalised mean bias ~~. The latter is given by~~

~~$$\mathrm{NMB}(\%) = 2\left\langle \frac{M-O}{M+O} \right\rangle \cdot 100\%,$$~~

(NMB):

$$\mathrm{STD(ppt)} \approx \left\langle (M - \langle M\rangle - O + \langle O\rangle)^2 \right\rangle^{1/2}, \tag{15}$$

$$\mathrm{Bias(ppt)} \approx \langle M - O\rangle, \tag{16}$$

$$\mathrm{NMB}(\%) \approx 2\left\langle \frac{M-O}{M+O} \right\rangle \cdot 100\%, \tag{17}$$

Tracer/ Kz scheme	loss rate, 10^3 mol/year	lifetime, years
passive, any Kz	0	∞
SF_6, ECMWF Kz	440	2900
SF_6, 0.001 Kz	480	2600
SF_6, 0.01 Kz	760	1700
SF_6, 0.03 Kz	800	1540
SF_6, 0.1 Kz	960	1300
SF_6, 1 Kz	2160	590

Table 1. SF_6 destruction rate after stopping emissions. Mid-2011 atmospheric burden of SF_6 of $1.27 \cdot 10^9$ moles is used as reference for the lifetime estimate

where M and O are modelled and observed values, respectively, and $\langle \cdot \rangle$ denotes averaging over the selected model-observation pairs for the given range of times and altitudes. Along with the STD, we have plotted the RMS error of the observations due to retrieval noise in the original MIPAS data, labeled as "MIPAS noise" in the top panels of Fig. 7 and Fig. 8.

In the altitude range of 10 – 35 km, the STD of model-measurement difference is ~~practically~~ uniform in time with minor peaks in August-September (Fig. 7). The level of the noise error constitutes about 85 % of the total model-measurement difference. Application of averaging kernel to the model profiles reduces the STD. The intermediate-diffusivity case "0.03Kz" clearly shows the least STD uniformly over the whole observation period, the same case indicates the least absolute bias.

In the range of 30 – 60 km altitudes (Fig. 8) the level of retrieval noise is noticeably higher than for the lower stratosphere. Unlike in the lower stratosphere, the least biased case is "1Kz", which has the largest STD. The STDs of "0.03Kz" and "0.001Kz" are ~~practically on pair~~on par, however the latter has the strongest biases. Thus for ~~the upper troposphere~~ this altitude range the intermediate-diffusivity case also shows the best performance.

4.4 Lifetime of SF_6 in the atmosphere

In order to estimate the atmospheric lifetime of SF_6 we turned off the emission of all simulated SF_6 tracers in July 2016 and let the model run until the end of 2018 without emissions (Fig. 9). The decrease of the simulated SF_6 burden after the emission stop can be used to estimate the SF_6 removal rate from the atmosphere.

Time series of the total burden of SF_6 in the atmosphere in the simulations are given in Fig. 9. For easier comparison to observed mixing ratios the burden has been normalised with $1.78 \cdot 10^{20}$ moles – the total amount of air in the atmosphere – to get the mean mixing ratio. The tabulated values for the atmospheric burden of SF_6 from Levin et al. (2010) and Rigby et al. (2010) are given for comparison. Since the removal of SF_6 from the atmosphere is mostly controlled by the transport towards the depletion layer, the vertical exchange is a key controlling factor. In all simulated cases, the removal of SF_6 from the atmosphere is very slow, so the relative difference between the cases is small. Similar rates could have been obtained by averaging the inverse destruction rate mass-weighted over the entire atmosphere.

The decrease of the atmospheric SF_6 content after the emission stop, is given at the zoom panel of Fig. 9. As expected, after July 2016 the content of passive SF_6 stays constant, while SF_6 that undergoes chemical destruction begins to decrease at a rate that depends on the transport properties of the stratosphere in the simulations, with faster removal for stronger eddy diffusivity. The removal rate is driven by the SF_6 content in the upper stratosphere, which is not in equilibrium with total atmospheric SF_6 content. A typical delay between SF_6 mixing ratio in the troposphere, where most of SF_6 resides, and the upper stratosphere, from where SF_6 escapes further to the depletion layers, i.e. AoA in the topmost model layer, is about 5-6 years. Hence, to estimate the SF_6 lifetimes we used the total amount of atmospheric SF_6 5 years before the emission stop, i.e. 1.23×10^9 mol , which corresponds to mean mixing ratio of about 7 pmol/mol. Dividing the destruction rate with the reference amount one gets the range of corresponding simulated SF_6 life times in the atmosphere: 600 to 2900 years. Despite the range of assumed diffusivities is three orders of magnitude, the loss rate of SF_6 varies within a factor of five (Table 1).

The term "life time" implies a linear decay, however, due to emissions the distribution of SF_6 in the atmosphere is far from equilibrium, so the decay is not proportional to the burden. A more accurate way to estimate life time would be to perform a multi-decade simulation without sources, to get the distribution of SF_6 into a quasi-equilibrium with the mesospheric sink. In such a quasi-equilibrium a model of linear decay of SF_6 in the whole atmosphere becomes applicable, and the life time can be estimated as a simple ratio of burden to the loss rate. The uncertainty in the equilibrium burden corresponding to the modelled loss rates in Table 1 can be estimated as the range of AoA in the upper stratosphere (~ 0.5 years) divided by the growth rate of the burden ($0.04\,\mathrm{year}^{-1}$), i.e about 2%. The major uncertainty comes from the over-simplistic parametrization of the SF_6 loss in the model, which is more difficult to quantify.

The best-performing in terms of SF_6 simulation resulted in 1540 years lifetime. Given the uncertainties above, it meets the ranges suggested by earlier studies. It is in a good agreement with the range of 800 – 3200 years from earlier model studies (Ravishankara et al., 1993; Morris et al., 1995), and is close to the upper bound of the 580–1400 years range recently obtained by (Ray et al., 2017) from the balloon profile given in Fig. 5b.

Our estimate is also slightly above the range given by Kovács et al. (2017), who obtained 1120 – 1475 years. Note, however, that in the simulations of Kovács et al. (2017) the mixing ratios of SF_6 in the stratosphere and lower mesosphere were noticeably higher than retrieved from MIPAS, which is likely to cause overstating the simulated depletion rates, and lead to corresponding low bias of the SF_6 lifetime from those simulations.

5 Simulations of AoA

5.1 Eddy diffusivity and simulated AoA

The effect of the vertical eddy diffusivity on AoA in the stratosphere was evaluated with the same set of three prescribed K_z profiles and one dynamic K_z profile, as for SF_6 simulations. An example of annual-mean distributions of AoA for the same year is given in Fig. 10. The Hunten (1975) K_z profile (Fig. 10a) gives AoA in the stratosphere of about 3.5 years. It is much shorter than available estimates of stratospheric AoA (e.g. Waugh, 2009; Engel et al., 2009) from the observations of various tracers. Three other profiles of K_z result in ~~practically identical~~ almost identical average distribution of AoA with typical

stratospheric AoA of 5.5 years, which agrees quite well with the experimental estimates. In these cases AoA is controlled by the transport with explicitly resolved winds. Since "0.03Kz" profiles result in most realistic distribution of SF_6 in our simulations, in the current section we will use simulated distributions of tracers with "0.03Kz" eddy diffusivity.

5.2 ~~Age-of-Air~~ AoA and apparent SF_6 AoA

The AoA for all tracers (except for the "ideal age") was calculated as a simple time lag between a mixing ratio in a given point of the domain and the mean near-surface mixing ratio. As it has been pointed out by (Waugh and Hall, 2002), this lag equals to AoA only in case of a fully passive tracer with linearly growing (or decreasing) near-surface mixing ratio. Corrections have been applied to the AoA derived from SF_6 in many studies studies (Volk et al., 1997; Stiller et al., 2008, 2012; Engel et al., 2009) to account for non-linear growth of the near-surface SF_6 mixing ratio and for mesospheric sink of it. The corrections rely heavily on various assumptions that can hardly be rigorously verified for the atmospheric circulation. Therefore in this study for the sake of simplicity we do not apply any corrections to the AoA derived from time lags of tracers. The corrections and assumptions behind them are discussed in Sec. 6.

The constant-rate emission of the "passive" tracer in our simulations resulted in ~~practically~~ nearly linear growth of the near-surface mixing ratio of the tracer after a decade of spin-up. The latter makes the age derived from the "passive" tracer equivalent to the age derived from the ideal-age tracer. The resulting distributions of "passive" and ideal-age AoA are indeed very close to each other (Fig. 11 a and b). The agreement confirms the self-consistency of the transport procedure since the tracers have opposite sensitivity to the advection errors: higher mixing ratios correspond to younger air for the accumulating tracers, while for the ideal-age tracer higher mixing ratios correspond to older air. The remaining differences of are caused by spatial inhomogeneities of near-surface mixing ratio of "passive"due to variations in the near-surface air density.

The distribution of the AoA derived from "sf6pass" (Fig. 11c) is ~~partly~~ similar to the ideal-age one, however one can see substantial differences. The negative AoA in northern troposphere for the "sf6pass" tracer is caused by the predominant location of the sources in the northern hemisphere, so the concentrations there exceed global-mean levels. The growing rate of the SF_6 emissions leads to the ~~greater than linear~~ greater-than-linear increase of near-surface mixing ratios, which leads to ~~a slight old bias~~ an old bias up to 3-5 months of the "sf6pass" AoA. This old bias has been one of the drawbacks of the SF_6 AoA pointed by Garcia et al. (2011).

The ages shown in Fig. 11a – c agree well with the ages derived from *in-situ* observations of SF_6 and CO_2 at the 25 km altitude by Waugh and Hall (2002). They also agree quite well with earlier simulations with five climate models that give annual mean ages in the upper stratosphere between 4.5 and 5.5 years (Butchart et al., 2010), and with Lagrangian simulations of (Diallo et al., 2012) driven by the same ERA-Interim meteorological fields as used for the present study. A substantial disagreement, however, exists with the ages derived from the MIPAS satellite observations (Stiller et al., 2012; Haenel et al., 2015), who calculated ages exceeding 10 years in polar areas and in the upper stratosphere. The reason for the disagreement follows from the above analysis: SF_6 can neither be considered as a passive tracer nor ~~its mixing ration~~ does its mixing ratio in the troposphere grows linearly with time. Denoting the AoA derived from the SF_6 profiles as "apparent AoA" (Waugh and Hall, 2002), we calculated it from the SILAM-predicted SF_6 profiles, which, as shown above, agree well ~~well~~ with AoA derived

from MIPAS. The resulting model-based apparent AoA (Fig. 11d) is indeed much older than the "ideal-age" AoA~~and pretty close to the values derived from MIPAS profiles by Stiller et al. (2012); Haenel et al. (2015)~~. The distribution of apparent SF_6 AoA agrees to the AoA from MIPAS SF_6 profiles by Haenel et al. (2015): well over 5 years AoA around equator with well over 10 years AoA in polar regions.

The effect of apparent over-aging in the stratosphere due to the subsidence of the mesospheric air was estimated by Stiller et al. (2012) to be a fraction of a year in the upper stratosphere. Earlier experimental balloon studies (Strunk et al., 2000) indicated up to 3.5-year difference between CO_2 and SF_6 ages. In our simulations, the over-aging due to the SF_6 depletion and other factors discussed in previous sections is much stronger and affects ~~practically~~ the whole stratosphere.

5.3 Trends in apparent AoA

Changes in AoA have been used in many studies as an indicator of changes in the atmospheric circulation. In order to evaluate the effect of the way AoA is evaluated on trends in AoA we have calculated trends in apparent AoA at different altitudes and latitudes for 11 years 2002-2012. This period roughly covers the MIPAS mission time and allows for comparison with trends reported by Haenel et al. (2015).

The zonal-mean vertical profiles of the AoA trends during 2002-2012 are shown in Fig. 12 for five latitudinal belts. The presented variable is a slope of the linear fit of ~~the AoA~~ deseasonalized monthly-mean time series for each tracer, averaged over the corresponding latitudinal belt and model layer. The fit was made with the ordinary least-squares method for each tracer. The error-bars show 95-% confidence intervals, calculated as if a model of linear trend with uncorrelated Gaussian noise was applicable to the time series.

The trends of the apparent AoA for the non-passive SF_6 species have a clear increase with height in the upper part of the profiles. The increase is the largest at high latitudes. Such a behaviour of trends agrees well with the AoA trends of Haenel et al. (2015, Fig. 7) obtained from the MIPAS observations. The over-aging due to the mesospheric depletion of SF_6 has been discussed and estimated by Haenel et al. (2015); Kovács et al. (2017). However, Fig. 12 shows that the mesospheric depletion of SF_6 also affects its trend: the over-aging increases with time. The reason is that depletion is proportional to the SF_6 load, which grows with time. This effect has been pointed out earlier by Stiller et al. (2012).

The apparent AoA derived with passive SF_6 tracer "sf6pass" indicates a negative trend of about 0.5 years/decade. The trend is caused by the temporal variation of SF_6 emissions. In order to get unbiased AoA estimate from a passive tracer, one needs the mixing ratio at the surface increasing linearly with time. A steady growth of emission rate at the surface leads to faster-than-linear increase of near-surface mixing ratio and, thus, low-bias of AoA since younger (i.e. more rich with SF_6) air gets more weight when two volumes of different age mix. According to the inventory (Levin et al., 2010) used in this study, the SF_6 emission rate was growing in 1997–2000 about twice slower than after 2005. Consequently, the negative bias of apparent AoA has increased resulting in negative trend if AoA in the stratosphere.

The AoA trends derived from the "ideal age" and "passive" tracers agree through the whole range of altitudes and latitudes indicating internal consistency of our simulations. The main common feature of the profiles is the negative tendency of about -0.5 year/decade in the altitude range of 15-30 km ~~. We suspect it to~~ with a profile that varies across altitudes.

Similar-magnitude trends for the same period were reported by Plöger et al. (2015), who used the same ERA-Interim to simulate AoA. The major difference between the obtained trends is that we have consistently negative trends for both hemispheres, whereas Plöger et al. (2015) indicate a positive trend of a fraction of year per decade in the altitude range of 20 – 30 km in the Northern hemisphere, and similar-magnitude negative trend in the Southern hemisphere. The reason for the discrepancy despite the same input dataset deserves further investigation.

The trends might be a feature of the non-uniformity of the ERA-Interim dataset, which was produced with assimilation of an inhomogeneous set of the observations. During ~~that period~~2002-2012, the amount of the assimilated data on the upper-air temperatures was by an order of magnitude higher than before 2000 and two orders of magnitude higher than after 2010 (Dee et al., 2011). It had a clear impact on the patterns of analysis increments in ERA-Interim and, consequently, on the predicted stratospheric circulation. Due to such inhomogeneities, the quality of trends derived from reanalysis data needs to be verified for each geophysical quantity (Dee et al., 2011). Deducing reliable trends for atmospheric temperature, quantity that is measurable and extensively assimilated, took a major effort (Simmons et al., 2014). The fact that AoA is not a directly observable quantity makes the verification of the AoA trends in ERA-Interim ~~was not recommended for climatological studies~~hardly possible.

To get more insight on the nature of the simulated long-term AoA variability at different altitudes and latitudes we have plotted the time series of monthly zonal-mean ideal-age AoA for the same latitude belts as in Fig. 12 over 1990-2018 (Fig. 13). To make the temporal variations more visible, the mean AoA profile for each latitude averaged over the same period was subtracted form the profiles. One can see a clear seasonal variation of the AoA outside of the equatorial zone. The variation has opposite phase between the upper and the lower stratosphere. In the altitude range of 20 – 30 km, where the trends are most pronounced, the temporal variation of AoA has a ramp structure with more-or-less steady intervals and relatively quick changes. Such structure is similar to the one shown for the ERA=Interim analysis increments (Dee et al., 2011) and is likely to be caused by temporal inhomogeneities in the assimilated dataset. Therefore we do not draw any conclusion here on the actual trends of AoA but highlight that ~~the trends of~~ trends of the apparent AoA are ~~completely determined~~ strongly influenced by selected time interval, and by the method of ~~its~~ trends calculation.

6 Discussion

The present study has several limitations that deserve specific attention. Forced zero air flux through the domain top at 0.1 hPa caused distortion of the mean transport within the domain, and left diffusive transport as the only means for the upper-boundary fluxes of SF_6. Moreover, we used prescribed profiles of the eddy diffusivity within the domain, which also affects the results of the simulations. In this section we evaluate the role of these distortions.

6.1 Distortions of air-flows

The transport procedure used in this study is done with a "hardtop" diagnostics forcing zero mass-fluxes at the domain top and forced air-mass conservation everywhere within the domain. Since the upper boundary of the domain is at 0.1 hPa, the divergence of the air flow above that level in the meteorological driver is compensated by adjusting the divergences within the

domain. To evaluate the effect of this adjustment on the mean circulations we used the ERA-5 data set, which has the topmost level at 1×10^{-3} hPa, as a reference. The diagnostic procedure was applied to ERA5 for two sets of vertical layers: the 61 ERA-Interim layers, same as used in SF_6 simulations (hereafter ERA5-cut), and a refined vertical matching 137 native ERA5 vertical layers (hereafter ERA5). The resulting vertical winds were compared to the ones used in the SF_6 simulations: 61 ERA-Interim layers diagnosed from ERA-Interim. The seasonal and zonal-mean vertical air-mass fluxes, expressed in units of Pa/day for the three cases and two solstice seasons of 2017 are shown in Fig. 14 together with corresponding layer boundaries.

The wind patterns in ERA5 (Fig. 14abde have finer features than in ERA-Interim due to the higher horizontal resolution of the former. The difference between the ERA5 and ERA5-cut vertical winds is strongest at the cut domain top (0.1 hPa, 65 km), where zero vertical air-mass flux is forced. For both seasons the disturbances introduced by the cut vertical to the ERA5 dataset below 55 km are minor, except for the summertime poles (South pole in Fig. 14ab, and North pole in Fig. 14de), where a noticeable disturbance is visible down to 35-40 km altitude. Such systematic disturbances influence the performance of the AoA and SF_6 simulations in the polar stratosphere, and they are a probable reason for the failure of the model to reproduce the SF_6 profiles there (see Fig. 6).

The comparison of the same-vertical mass-fluxes (panels b vs. c, or e vs. f in Fig. 14) shows that the difference between ERA-Interim and ERA5 is noticeably larger than between cut- and full vertical of ERA5. Thus we conclude that the distortions introduced by our diagnostic procedure are within the uncertainty of the input meteorological data.

6.2 Top-boundary mass fluxes and eddy diffusion profiles

The used modelling approach replaces the vertical transport through the domain top with diffusive fluxes for depleting SF_6 and a hard lid for other species. One can hope that the approach does not introduce any major disturbances into the AoA fields, since AoA is quite uniform close to the domain top. The uncertainty introduced with this approach into the SF_6 fields is not straightforward to evaluate due to a major uncertainty in the vertical diffusivity profiles.

As mentioned in Sec. 3.2, the eddy diffusivity profiles of the C-IFS model form the ERA5 reanalysis (Fig. 2) are clearly unrealistic within and above the stratosphere. They do not exhibit any growth of the eddy diffusivity in the mesosphere due to breaking gravity waves. According to Lindzen (1981) the mean diffusivity due to the breaking has an order of magnitude of $1 \times 10^2\,\mathrm{m}^2/\mathrm{s}$, whereas the eddy diffusion in ERA5 for that region is below the molecular diffusivity (Fig. 2). On the other hand, if we assume that the mesospheric turbulence due to the breaking gravity waves results in a diffusivity profile as predicted by Lindzen (1981) (Fig. 2), then such a turbulence provides quite rapid exchange of SF_6 towards depletion layers making the advective vertical transport above $\sim 50\,\mathrm{km}$ negligible. The profiles of (Lindzen, 1981), however do not allow for a simple extrapolation to below 50 km, and therefore the vertical profiles by Massie and Hunten (1981) ("1Kz") were involved as the ones that are simple to implement and smooth enough to be easily approximated and extrapolated. The scaling of the "1Kz" profile allowed for the sensitivity tests.

The normalized diffusive SF_6 mass-fluxes above the domain top for the scaled profiles of the eddy diffusivity (Fig. 3) allow for evaluation of the validity of the assumption of neglected regular vertical transport above the domain top. The equivalent

vertical air-mass flux due to diffusion at the level of 0.1 hPa (domain top) is 6×10^{-6}, 9×10^{-7}, and 2.5×10^{-7} kg/m^2/s for "1Kz", "0.03Kz", and "0.001Kz" correspondingly. These mass fluxes, divided by g give the vertical velocities of -5, -0.8, and -0.4 Pa/day. Comparing these values to those shown in Fig. 2 for the level of 65 km, one can see that the diffusive limit is valid for the "1Kz" profile except for the very vicinities of the poles. For lower values of the eddy diffusivity the regular circulation becomes comparable with the diffusion or even exceed it.

Although the "0.03Kz" profiles gave somewhat better agreement with the observations of SF_6, this does not indicate that "0.03Kz" profiles are more realistic. As suggested by one of the anonymous reviewers, this profile is likely to over-mix the lower stratosphere and under-mix the upper stratosphere and the mesosphere. Thus the vertical structure of the eddy diffusivity remains a major source of uncertainty in the modelling approach. Using more realistic vertical diffusion profiles and high-top ERA5 reanalysis is planned for the future studies.

6.3 Notes on the observed SF_6-age

There are three main factors that are responsible for SF_6 age being different form the "ideal age": the non-linear growth of tropospheric burden, the gravitational separation, and the mesospheric sink. Here we consider the effects of these factors and corrections to the SF_6 observations that can be applied to compensate for the effect of these factors on resulting AoA.

The correction for the non-linear growth rate introduced by Volk et al. (1997) and used in many subsequent studies is based on a simple analytical model of 1D diffusion with constant diffusivity and exponential distribution of air density. The model was suggested by (Hall and Plumb, 1994) as an illustration for the concept of the age spectrum. The model spectrum has two parameters: the mean age Γ and the width parameter Δ. In order to use the spectrum for the correction one has to involve an additional constraint connecting these parameters. Based on a 3D simulation with a general circulation model Hall and Plumb (1994) suggested that a constant ratio $\Delta^2/\Gamma = 0.7$ year can be used throughout the stratosphere. Note that this dimensional parameter, while having proper units originally, appears without units in several subsequent papers (Engel et al., 2002; Stiller e . Volk et al. (1997) used the value $\Delta^2/\Gamma = (1.25 \pm 0.50)$ year for the lower stratosphere based on the results of a more advanced GCM than the one used by (Hall and Plumb, 1994). With this approach Volk et al. (1997) obtained the difference between the mean age and the lag time (apparent SF_6 age). The difference becomes significant for air older than 3-4 years and approaches (0.50 ± 0.25) years for the oldest (6 years) air measured, which agrees quite well with the difference between the ideal age and the passive SF_6 in our simulations shown in Fig. 11bc. The correction for this difference derived from the 1D has been used to reduce systematic biases from SF_6-based AoA, though"the global stratosphere is poorly represented by a 1-D model" (Waugh and Hall, 2002). The uncertainty of the correction of up to ± 0.5 years is systematic, and is not guaranteed to be uniform in space or in time, and likely to affect the trend estimates.

As shown in Sec. 4.1, the biases introduced to the SF_6-based AoA by gravitational separation reach a fraction of a year in the upper stratosphere. One could in principle elaborate a correction for gravitational separation; however, the correction would be well within the uncertainty of the correction for the non-linear growth rate, and thus probably not worth considering.

The mesospheric sink clearly has the largest impact on the SF_6-derived AoA. The effect of the mesospheric sink is clearly visible above 15-20 km at all latitudes (Fig. 11), and leads to a factor of times apparent over-aging in the upper layers, especially

in polar areas. The effect of the sink alone can explain the discrepancy between AoA derived from the MIPAS observations (Haenel et al., 2015) and the AoA from modelling studies (e.g. Diallo et al., 2012; Brinkop and Jöckel, 2019). Compensating for such over-aging is hardly possible without detailed modelling of physical processes including depletion, diffusion and mean transport, which cause the over-aging. Since the AoA is derived as a *difference* of SF_6 mixing ratios, whereas depletion introduces *multiplicative* change to the SF_6 abundance, the effect of the sink on apparent SF_6 AoA is unsteady in time. This effect is clearly seen in Fig. 12.

Once one has a model that is capable of reproducing the processes behind the SF_6 depletion, it makes a full sense to validate such a model directly against available SF_6 observations, rather than deriving AoA from SF_6 observations and comparing it against modelled one. In any case the AoA derived from SF_6 tracer observations with all the needed corrections applied cannot be considered as purely observed one.

7 Conclusions

Eulerian simulations of the tropospheric and stratospheric transport of several tracers were performed with SILAM model driven by ERA-Interim reanalysis for 1980-2018. The simulations included several species representing SF_6 under different assumptions, a passive tracer emitted uniformly at the surface, and an "ideal age" tracer directly comparable ~~with Lagrangian simulations of a particle residence time~~are comparable to other state-of-the-art CTM simulations of AoA. To our best knowledge this is the first systematic evaluation of AoA derived from several different tracers within the same simulation over several decades, combined with extensive evaluation against MIPAS and balloon SF_6 observations.

Due to the limited vertical coverage and resolution of ERA-Interim in the upper stratosphere, the SILAM simulation domain had a lid at ~~10 Pa~~0.1 hPa, which is below the altitude of the SF_6 destruction. In order to perform realistic simulations of SF_6 in our setup, the eddy diffusion in the upper ~~troposphere~~ stratosphere and lower mesosphere had to be parameterised, along with the mesospheric sink of SF_6.

A set of simulations with different parameterisations for the vertical eddy diffusion showed that published profiles derived with no account for advection (see e.g. Massie and Hunten, 1981, and references threrin) overestimate the eddy diffusivity. On other hand, the eddy-diffusivity profiles for scalars calculated from ERA-Interim fields according to the IFS procedures ECMWF (2015)), or readily available from the ERA5 reanalysis, appear to be of no relevance for the upper stratosphere, since they fall below the molecular diffusivity. Evaluation of our simulations against satellite and balloon observations indicated that the best agreement between simulated and observed SF_6 mixing ratios within the model domain is achieved for the tabulated eddy-diffusivity profile of Hunten (1975) scaled down with a factor of 30. ~~It is not clear~~Note, however, ~~if~~ that this conclusion is ~~valid beyond the specific~~ likely to be a feature the specific model setup. Thus, the question ~~on~~ of the importance and magnitude of the eddy diffusivity in the upper stratosphere and lower mesosphere remains open~~. Our simulations indicate that the diffusivities of 0.1 m/s^2 or less can be used in the upper stratosphere, until the molecular diffusivity takes over~~, and SF_6 observations is a good means to validate more sophisticated parametrizations of it.

The mesospheric sink of SF_6 has a major impact on the mixing ratios above 20 km. The depletion impact is especially strong in wintertime polar areas due to the downdraft within a polar vortex. ~~The sensitivity tests have shown~~ A set of sensitivity tests showed that molecular diffusion and gravitational separation of SF_6 are responsible for up to a few percent of further reduction in SF_6 mixing ratios in the upper stratosphere.

A good agreement of the simulated SF_6 distribution to the MIPAS observations up to the altitudes of ~~30-40~~30-35 km and to available balloon profiles was shown. The standard deviation between MIPAS and modelled SF_6 mixing ~~rations~~ ratios is up to 80 % controlled by noise error of the satellite retrievals, i.e. the standard deviation between model and MIPAS is about as large as the error on the satellite data. The results of the comparison also underline the importance of accurate collocation of model and observed data in terms of space, time and vertical averaging of observed data.

The lifetime of SF_6 in the atmosphere estimated from the best-performing setup is about 1500 years, ~~in a good agreement with previous studies~~which is at the high side of the range of other recent estimates. Our estimate is likely to be biased high due to underrepresented vertical exchange to at the domain top due to missing advective transport and missing effect of braking gravity waves.

Our simulations were able to reproduce both AoA obtained in other model studies, and the apparent SF_6 AoA derived from the MIPAS observations. This highlights the role of fast mesospheric destruction of SF_6 due to the electron attachment mechanism. Having all tracers within the same simulations we were able to trace the differences in the estimated AoA to the peculiarities of each tracer. A good agreement of the passive-tracer and "ideal-age" AoA indicates a consistency of the simulations, since these two methods have opposite sign of sensitivity to errors of the transport scheme.

The mesospheric sink has severe implications on the AoA derived form SF_6. The apparent over-aging introduced by the sink is large and variable in space and season. Moreover, the over-aging due to the sink increases as the atmospheric burden of SF_6 grows. All this makes SF_6 unsuitable to infer AoA above ~ 20 km. ~~Even in for the~~ For a fully-passive SF_6 tracer~~there are deviations of apparent AoA from the "ideal-age" AoA caused by~~ , the variable rate of ~~the emissions~~ emissions causes deviations from the "ideal age", and these deviations can be compensated to some extent. However, the correcting for the deviations due to the mesospheric sink of SF_6 is hardly possible ithout detailed modeling. These deviations appear as long-term trends in the apparent AoA~~that differ from~~ . These trends differ from the trends in the "ideal-age AoA", and have ~~little relation~~ no direct correspondence to actual trends in the atmospheric circulation.

Procedures used to derive AoA from observations of various tracers in the atmosphere are inevitably based on assumptions and idealisations that have limited and often unknown area of applicability. The resulting uncertainties in AoA are large enough to preclude the use of apparent AoA and its trends for evaluation of changes in atmospheric circulation or for validation of atmospheric models. Observations of the tracers themselves, however, have quite well quantified uncertainties, so direct comparisons of simulated tracers to the observed ones are a very promising means for the atmospheric model evaluation. AoA in turn is a convenient means for model inter-comparison if a protocol of AoA derivation is well specified.

Code and data availability. The SILAM source code as well as the simulation results used for this study are available from MS or RK on request. The MIPAS observational data available from GS on request. ERA-Interim and ERA5 reanalyses data sets are available from the European Center for Medium-range weather forecast http://www.ecmwf.int.

Author contributions. RK performed the simulations and data analyses, prepared text and illustrations. MS and JV inspired the study and helped with discussions on content and structure of the study, and participated in editing the text. GS provided MIPAS data and wrote sections about MIPAS observations. All authors participated in the final preparation of the text.

Competing interests. The authors declare no competing interests.

Acknowledgements. The authors acknowledge the support of projects: EU FP7-MarcoPolo (ID: 606953), ESA-ATILA (contract no. 4000105828/12/F/MO and ASTREX of Academy of Finland (grant 139126), Russian Foundation for Basic Research (project 19-05-01008).

The SF_6 and mean age-of-air distributions from MIPAS observations were generated within the project STI 210/5-3 of the CAWSES priority program, funded by the German Research Foundation (DFG), and the project BDCHANGE (01LG1221B), funded by the German Federal Ministry of Education and Research (BMBF) within the "ROMIC" program.

The authors are grateful to Viktoria Sofieva (Finnish Meteorological institute) for reading the manuscript and providing useful comments, to Florian Haenel and Michael Kiefer (Karlsruhe Institute of Technology) for technical assistance in handling MIPAS SF_6 data, and to four anonymous reviewers whose very instrumental comments helped to substantially improve the paper.

References

Allen, M., Yung, Y. L., and Waters, J. W.: Vertical transport and photochemistry in the terrestrial mesosphere and lower thermosphere (50–120 km), J. Geophys. Res., 86, 3617–3627, https://doi.org/10.1029/JA086iA05p03617, 1981.

Andrews, A. E., Boering, K. A., Daube, B. C., Wofsy, S. C., Loewenstein, M., Jost, H., Podolske, J. R., Webster, C. R., Herman, R. L., Scott, D. C., and et al.: Mean ages of stratospheric air derived from in situ observations of CO2, CH4, and N2O, J. Geophys. Res., 106, 32 295–32 314, https://doi.org/10.1029/2001jd000465, 2001.

Bhandari, N., Lal, D., and Rama, D.: Stratospheric circulation studies based on natural and artificial radioactive tracer elements, Tellus, 18, 391–406, https://doi.org/10.1111/j.2153-3490.1966.tb00250.x, 1966.

Boering, K., Wofsy, S., Daube, B., Schneider, H., Loewenstein, M., Podolske, J., and Conway, T.: Stratospheric mean ages and transport rates from observations of carbon dioxide and nitrous oxide, Science, 274, 1340–1343, https://doi.org/10.1126/science.274.5291.1340, 1996.

Brinkop, S. and Jöckel, P.: ATTILA 4.0: Lagrangian advective and convective transport of passive tracers within the ECHAM5/MESSy chemistry–climate model, Geoscientific Model Development, 12, 1991–2008, 2019.

Butchart, N., Cionni, I., Eyring, V., Shepherd, T. G., Waugh, D. W., Akiyoshi, H., Austin, J., Brühl, C., Chipperfield, M. P., Cordero, E., and et al.: Chemistry–Climate Model Simulations of Twenty-First Century Stratospheric Climate and Circulation Changes, J. Climate, 23, 5349–5374, https://doi.org/10.1175/2010jcli3404.1, 2010.

Copernicus Climate Change Service (C3S): ERA5: Fifth generation of ECMWF atmospheric reanalyses of the global climate, Copernicus Climate Change Service Climate Data Store (CDS), 2018, https://cds.climate.copernicus.eu/cdsapp#!/home, 2017.

Cussler, E. L.: Diffusion: Mass Transfer in Fluid Systems (Cambridge Series in Chemical Engineering), Cambridge University Press, 1997.

Dee, D. P., Uppala, S. M., Simmons, A. J., Berrisford, P., Poli, P., Kobayashi, S., Andrae, U., Balmaseda, M. A., Balsamo, G., Bauer, P., and et al.: The ERA-Interim reanalysis: configuration and performance of the data assimilation system, Q. J. Roy. Meteorol. Soc., 137, 553–597, https://doi.org/10.1002/qj.828, 2011.

Diallo, M., Legras, B., and Chédin, A.: Age of stratospheric air in the ERA-Interim, Atmos. Chem. Phys., 12, 12 133–12 154, https://doi.org/10.5194/acp-12-12133-2012, 2012.

ECMWF: IFS Documentation – Cy41r1, Part 4: Physical processes, Tech. rep., European Center for Medium-range Weather Forecasts, http://old.ecmwf.int/publications/library/do/references/list/151, 2015.

Eluszkiewicz, J., Hemler, R. S., Mahlman, J. D., Bruhwiler, L., and Takacs, L. L.: Sensitivity of Age-of-Air Calculations to the Choice of Advection Scheme, J. Atmos. Sci., 57, 3185–3201, https://doi.org/10.1175/1520-0469(2000)057<3185:SOAOAC>2.0.CO;2, 2000.

Engel, A., Strunk, M., Müller, M., Haase, H.-P., Poss, C., Levin, I., and Schmidt, U.: Temporal development of total chlorine in the high-latitude stratosphere based on reference distributions of mean age derived from CO2 and SF6, Journal of Geophysical Research: Atmospheres, 107, ACH–1, 2002.

Engel, A., Möbius, T., Haase, H.-P., Bönisch, H., Wetter, T., Schmidt, U., Levin, I., Reddmann, T., Oelhaf, H., Wetzel, G., et al.: Observation of mesospheric air inside the arctic stratospheric polar vortex in early 2003, Atmospheric Chemistry and Physics, 6, 267–282, https://doi.org/1680-7324/acp/2006-6-267, 2006.

Engel, A., Möbius, T., Bönisch, H., Schmidt, U., Heinz, R., Levin, I., Atlas, E., Aoki, S., Nakazawa, T., Sugawara, S., and et al.: Age of stratospheric air unchanged within uncertainties over the past 30 years, Nature Geosci, 2, 28–31, https://doi.org/10.1038/ngeo388, 2009.

Engel, A., Rigby, M., Burkholder, J., Fernandez, R., Froidevaux, L., Hall, B., Hossaini, R., Saito, T., Vollmer, M., and Yao, B.: Update on Ozone-Depleting Substances (ODSs) and Other Gases of Interest to the Montreal Protocol, Chapter 1 in Scientific Assessment of Ozone

Depletion: 2018, Report 58, World Meteorological Organization, Geneva, Switzerland, https://www.esrl.noaa.gov/csd/assessments/ozone/2018/, 2018.

England, M. H.: The age of water and ventilation timescales in a global ocean model, Journal of Physical Oceanography, 25, 2756–2777, https://doi.org/10.1175/1520-0485(1995)025<2756:TAOWAV>2.0.CO;2, 1995.

Garcia, R. R., Randel, W. J., and Kinnison, D. E.: On the determination of age of air trends from atmospheric trace species, Journal of the Atmospheric Sciences, 68, 139–154, https://doi.org/10.1175/2010JAS3527.1, 2011.

Garny, H., Birner, T., Bönisch, H., and Bunzel, F.: The effects of mixing on age of air, Journal of Geophysical Research: Atmospheres, 119, 7015–7034, 2014.

Gavrilov, N. M., Luce, H., Crochet, M., Dalaudier, F., and Fukao, S.: Turbulence parameter estimations from high-resolution balloon temperature measurements of the MUTSI-2000 campaign, Annales Geophysicae, 23, 2401–2413, https://doi.org/10.5194/angeo-23-2401-2005, 2005.

Haenel, F. J., Stiller, G. P., von Clarmann, T., Funke, B., Eckert, E., Glatthor, N., Grabowski, U., Kellmann, S., Kiefer, M., Linden, A., and Reddmann, T.: Reassessment of MIPAS age of air trends and variability, Atmospheric Chemistry and Physics Discussions, 15, 14 685–14 732, https://doi.org/10.5194/acpd-15-14685-2015, 2015.

Hall, T. M. and Plumb, R. A.: Age as a diagnostic of stratospheric transport, J. Geophys. Res., 99, 1059–1070, https://doi.org/10.1029/93JD03192, 1994.

Hall, T. M., Waugh, D. W., Boering, K. A., and Plumb, R. A.: Evaluation of transport in stratospheric models, Journal of Geophysical Research: Atmospheres, 104, 18 815–18 839, 1999.

Harrison, J. J.: New and improved infrared absorption cross sections for trichlorofluoromethane (CFC-11), Atmospheric Measurement Techniques, 11, 5827–5836, https://doi.org/10.5194/amt-11-5827-2018, 2018.

Heimann, M. and Keeling, C. D.: A three-dimensional model of atmospheric ~~CO_2~~ CO2 transport based on observed winds: 2. ~~Model~~ Model description and simulated tracer experiments, pp. 237–275, American Geophysical Union (AGU), https://doi.org/10.1029/GM055p0237, 1989.

Hunten, D. M.: Estimates of Stratospheric Pollution by an Analytic Model, Proceedings of the National Academy of Sciences of the United States of America, 72, 4711–4715, http://www.jstor.org/stable/65270, 1975.

IPCC: Climate Change 2013: The Physical Science Basis. Contribution of Working Group I to the Fifth Assessment Report of the Intergovernmental Panel on Climate Change, Cambridge University Press, Cambridge, United Kingdom and New York, NY, USA, https://doi.org/10.1017/CBO9781107415324, www.climatechange2013.org, 2013.

Ishidoya, S., Sugawara, S., Morimoto, S., Aoki, S., and Nakazawa, T.: Gravitational separation of major atmospheric components of nitrogen and oxygen in the stratosphere, Geophysical Research Letters, 35, https://doi.org/10.1029/2007gl030456, 2008.

Ishidoya, S., Sugawara, S., Morimoto, S., Aoki, S., Nakazawa, T., Honda, H., and Murayama, S.: Gravitational separation in the stratosphere–a new indicator of atmospheric circulation, Atmospheric Chemistry and Physics, 13, 8787–8796, 2013.

Jacob, D. J., Prather, M. J., Rasch, P. J., Shia, R.-L., Balkanski, Y. J., Beagley, S. R., Bergmann, D. J., Blackshear, W. T., Brown, M., Chiba, M., Chipperfield, M. P., de Grandpré, J., Dignon, J. E., Feichter, J., Genthon, C., Grose, W. L., Kasibhatla, P. S., Köhler, I., Kritz, M. A., Law, K., Penner, J. E., Ramonet, M., Reeves, C. E., Rotman, D. A., Stockwell, D. Z., Van Velthoven, P. F. J., Verver, G., Wild, O., Yang, H., and Zimmermann, P.: Evaluation and intercomparison of global atmospheric transport models using 222Rn and other short-lived tracers, Journal of Geophysical Research: Atmospheres, 102, 5953–5970, https://doi.org/10.1029/96JD02955, 1997.

Koch, D. and Rind, D.: Beryllium 10/beryllium 7 as a tracer of stratospheric transport, Journal of Geophysical Research: Atmospheres, 103, 3907–3917, https://doi.org/10.1029/97JD03117, 1998.

Kovács, T., Feng, W., Totterdill, A., Plane, J. M. C., Dhomse, S., Gómez-Martín, J. C., Stiller, G. P., Haenel, F. J., Smith, C., Forster, P. M., García, R. R., Marsh, D. R., and Chipperfield, M. P.: Determination of the atmospheric lifetime and global warming potential of sulfur hexafluoride using a three-dimensional model, Atmospheric Chemistry and Physics, 17, 883–898, https://doi.org/10.5194/acp-17-883-2017, 2017.

Krol, M., de Bruine, M., Killaars, L., Ouwersloot, H., Pozzer, A., Yin, Y., Chevallier, F., Bousquet, P., Patra, P., Belikov, D., Maksyutov, S., Dhomse, S., Feng, W., and Chipperfield, M. P.: Age of air as a diagnostic for transport timescales in global models, Geoosci. Model Devel., 11, 3109–3130, https://doi.org/10.5194/gmd-11-3109-2018, 2018.

Leedham Elvidge, E., Bönisch, H., Brenninkmeijer, C. A., Engel, A., Fraser, P. J., Gallacher, E., Langenfelds, R., Mühle, J., Oram, D. E., Ray, E. A., et al.: Evaluation of stratospheric age of air from CF_4, C_2F_6, C_3F_8, CHF_3, HFC-125, HFC-227ea and SF_6; implications for the calculations of halocarbon lifetimes, fractional release factors and ozone depletion potentials, Atmospheric Chemistry and Physics, 18, 3369–3385, https://doi.org/10.5194/acp-18-3369-2018, 2018.

Legras, B., Pisso, I., Berthet, G., and Lefèvre, F.: Variability of the Lagrangian turbulent diffusion in the lower stratosphere, Atmos. Chem. Phys., 5, 1605–1622, https://doi.org/10.5194/acp-5-1605-2005, 2005.

Levin, I., Naegler, T., Heinz, R., Osusko, D., Cuevas, E., Engel, A., Ilmberger, J., Langenfelds, R. L., Neininger, B., Rohden, C. v., et al.: The global SF6 source inferred from long-term high precision atmospheric measurements and its comparison with emission inventories, Atmospheric Chemistry and Physics, 10, 2655–2662, https://doi.org/10.5194/acp-10-2655-2010, 2010.

Li, S. and Waugh, D. W.: Sensitivity of mean age and long-lived tracers to transport parameters in a two-dimensional model, Journal of Geophysical Research: Atmospheres, 104, 30 559–30 569, https://doi.org/10.1029/1999JD900913, 1999.

Lindzen, R. S.: Turbulence and stress owing to gravity wave and tidal breakdown, Journal of Geophysical Research: Oceans, 86, 9707–9714, https://doi.org/10.1029/JC086iC10p09707, 1981.

Mange, P.: The theory of molecular diffusion in the atmosphere, Journal of Geophysical Research, 62, 279–296, 1957.

Marrero, T. R. and Mason, E. A.: Gaseous diffusion coefficients, Journal of Physical and Chemical Reference Data, 1, 3–118, https://doi.org/10.1063/1.3253094, 1972.

Massie, S. T. and Hunten, D. M.: Stratospheric eddy diffusion coefficients from tracer data, J. Geophys. Res., 86, 9859–9867, https://doi.org/10.1029/jc086ic10p09859, 1981.

Monge-Sanz, B. M., Chipperfield, M. P., Dee, D. P., Simmons, A. J., and Uppala, S. M.: Improvements in the stratospheric transport achieved by a chemistry transport model with ECMWF (re)analyses: identifying effects and remaining challenges, Q. J. Roy. Meteorol. Soc., 139, 654–673, https://doi.org/10.1002/qj.1996, 2012.

Moore, F., Elkins, J., Ray, E., Dutton, G., Dunn, R., Fahey, D., McLaughlin, R., Thompson, T., Romashkin, P., Hurst, D., et al.: Balloonborne in situ gas chromatograph for measurements in the troposphere and stratosphere, Journal of Geophysical Research: Atmospheres, 108, https://doi.org/1029/2001JD000961, 2003.

Morris, R. A., Miller, T. M., Viggiano, A., Paulson, J. F., Solomon, S., and Reid, G.: Effects of electron and ion reactions on atmospheric lifetimes of fully fluorinated compounds, Journal of Geophysical Research: Atmospheres, 100, 1287–1294, 1995.

NOAA, NASA, and USAF: U.S. Standard Atmosphere, U.S. Governement Printing Office, Washington D.C., 1976.

Osman, M., Hocking, W., and Tarasick, D.: Parameterization of large-scale turbulent diffusion in the presence of both well-mixed and weakly mixed patchy layers, Journal of Atmospheric and Solar-Terrestrial Physics, 143-144, 14–36, https://doi.org/10.1016/j.jastp.2016.02.025, 2016.

Patra, P. K., Lal, S., Subbaraya, B., Jackman, C. H., and Rajaratnam, P.: Observed vertical profile of sulphur hexafluoride (SF6) and its atmospheric applications, Journal of Geophysical Research: Atmospheres, 102, 8855–8859, https://doi.org/10.1029/96JD03503, 1997.

Patra, P. K., Houweling, S., Krol, M., Bousquet, P., Belikov, D., Bergmann, D., Bian, H., Cameron-Smith, P., Chipperfield, M. P., Corbin, K., et al.: TransCom model simulations of CH 4 and related species: linking transport, surface flux and chemical loss with CH 4 variability in the troposphere and lower stratosphere, Atmospheric Chemistry and Physics, 11, 12 813–12 837, https://doi.org/10.5194/acp-11-12813-2011, 2011.

Pisso, I. and Legras, B.: Turbulent vertical diffusivity in the sub-tropical stratosphere, Atmos. Chem. Phys., 8, 697–707, https://doi.org/10.5194/acp-8-697-2008, 2008.

Plöger, F., Abalos, M., Birner, T., Konopka, P., Legras, B., Müller, R., and Riese, M.: Quantifying the effects of mixing and residual circulation on trends of stratospheric mean age of air, Geophysical Research Letters, 42, 2047–2054, https://doi.org/10.1002/2014GL062927, 2015.

Ravishankara, A. ~~R.~~, Solomon, S., Turnipseed, A. ~~A.~~, and Warren, R. ~~F.~~: Atmospheric lifetimes of long-lived halogenated species, Science, 259, 194–199, ~~,~~ 1993.

Ray, E. A., Moore, F. L., Elkins, J. W., Hurst, D. F., Romashkin, P. A., Dutton, G. S., and Fahey, D. W.: Descent and mixing in the 1999–2000 northern polar vortex inferred from in situ tracer measurements, Journal of Geophysical Research: Atmospheres, 107, https://doi.org/10.1029/2001JD000961, 2002.

Ray, E. A., Moore, F. L., Rosenlof, K. H., Davis, S. M., Sweeney, C., Tans, P., Wang, T., Elkins, J. W., Bönisch, H., Engel, A., et al.: Improving stratospheric transport trend analysis based on SF6 and CO2 measurements, Journal of Geophysical Research: Atmospheres, 119, 14–110, https://doi.org/10.1002/2014JD021802, 2014.

Ray, E. A., Moore, F. L., Elkins, J. W., Rosenlof, K. H., Laube, J. C., Röckmann, T., Marsh, D. R., and Andrews, A. E.: Quantification of the SF6 lifetime based on mesospheric loss measured in the stratospheric polar vortex, Journal of Geophysical Research: Atmospheres, 122, 4626–4638, https://doi.org/10.1002/2016JD026198, 2017.

Reddmann, T., Ruhnke, R., and Kouker, W.: Three-dimensional model simulations of SF6 with mesospheric chemistry, Journal of Geophysical Research: Atmospheres, 106, 14 525–14 537, https://doi.org/10.1029/2000JD900700, 2001.

Remsberg, E. E.: Methane as a diagnostic tracer of changes in the Brewer-Dobson circulation of the stratosphere, Atmos. Chem. Phys., 15, 3739–3754, https://doi.org/10.5194/acp-15-3739-2015, 2015.

Rigby, M., Mühle, J., Miller, B. R., Prinn, R. G., Krummel, P. B., Steele, L. P., Fraser, P. J., Salameh, P. K., Harth, C. M., Weiss, R. F., and et al.: History of atmospheric SF6 from 1973 to 2008, Atmos. Chem. Phys., 10, 10 305–10 320, https://doi.org/10.5194/acp-10-10305-2010, 2010.

Simmons, A., Poli, P., Dee, D., Berrisford, P., Hersbach, H., Kobayashi, S., and Peubey, C.: Estimating low-frequency variability and trends in atmospheric temperature using ERA-Interim, Quarterly Journal of the Royal Meteorological Society, 140, 329–353, https://doi.org/10.1002/qj.2317, 2014.

Smith, A. K., Garcia, R. R., Marsh, D. R., and Richter, J. H.: WACCM simulations of the mean circulation and trace species transport in the winter mesosphere, Journal of Geophysical Research: Atmospheres, 116, https://doi.org/10.1029/2011JD016083, 2011.

Sofiev, M., Vira, J., Kouznetsov, R., Prank, M., Soares, J., and Genikhovich, E.: Construction of the SILAM Eulerian atmospheric dispersion model based on the advection algorithm of Michael Galperin, Geoosci. Model Devel., 8, 3497–3522, https://doi.org/10.5194/gmd-8-3497-2015, 2015.

Stiller, G. P., von Clarmann, T., Höpfner, M., Glatthor, N., Grabowski, U., Kellmann, S., Kleinert, A., Linden, A., Milz, M., Reddmann, T., Steck, T., Fischer, H., Funke, B., López-Puertas, M., and Engel, A.: Global distribution of mean age of stratospheric air from MIPAS SF_6 measurements, Atmos. Chem. Phys., 8, 677–695, https://doi.org/10.5194/acp-8-677-2008, 2008.

Stiller, G. P., von Clarmann, T., Haenel, F., Funke, B., Glatthor, N., Grabowski, U., Kellmann, S., Kiefer, M., Linden, A., Lossow, S., and Lopez-Puertas, M.: Observed temporal evolution of global mean age of stratospheric air for the 2002 to 2010 period, Atmos. Chem. Phys., 12, 3311–3331, https://doi.org/10.5194/acp-12-3311-2012, 2012.

Strunk, M., Engel, A., Schmidt, U., Volk, C. M., Wetter, T., Levin, I., and Glatzel-Mattheier, H.: CO2 and SF6 as stratospheric age tracers: Consistency and the effect of mesospheric SF6-loss, Geophysical Research Letters, 27, 341–344, https://doi.org/10.1029/1999GL011044, 2000.

Sugawara, S., Ishidoya, S., Aoki, S., Morimoto, S., Nakazawa, T., Toyoda, S., Inai, Y., Hasebe, F., Ikeda, C., Honda, H., et al.: Age and gravitational separation of the stratospheric air over Indonesia, Atmospheric Chemistry and Physics, 18, 1819–1833, 2018.

Thiele, G. and Sarmiento, J. L.: Tracer dating and ocean ventilation, Journal of Geophysical Research: Oceans, 95, 9377–9391, https://doi.org/10.1029/JC095iC06p09377, 1990.

Totterdill, A., Kovács, T., Gómez Martín, J. C., Feng, W., and Plane, J. M. C.: Mesospheric Removal of Very Long-Lived Greenhouse Gases SF6 and CFC-115 by Metal Reactions, Lyman-α Photolysis, and Electron Attachment, The Journal of Physical Chemistry A, 119, 2016–2025, https://doi.org/10.1021/jp5123344, 2015.

Varanasi, P., Li, Z., Nemtchinov, V., and Cherukuri, A.: Spectral absorption-coefficient data on HCFC-22 and SF_6 for remote-sensing applications, Journal of Quantitative Spectroscopy and Radiative Transfer, 52, 323–332, https://doi.org/10.1016/0022-4073(94)90162-7, 1994.

~~Waugh~~

Volk, C. M., Elkins, J. W., Fahey, D.~~: Age of stratospheric air: Theory, observations, and models, Reviews of Geophysics, 40, , 2002.~~ W., Dutton, G. S., Gilligan, J. M., Loewenstein, M., Podolske, J. R., Chan, K. R., and Gunson, M. R.: Evaluation of source gas lifetimes from stratospheric observations, Journal of Geophysical Research: Atmospheres, 102, 25 543–25 564, https://doi.org/10.1029/97JD02215, 1997.

Waugh, D.: Atmospheric dynamics: The age of stratospheric air, Nature Geosci, 2, 14–16, https://doi.org/10.1038/ngeo397, 2009.

Waugh, D. W. and Hall, T. M.: Age of stratospheric air: Theory, observations, and models, Reviews of Geophysics, 40, https://doi.org/10.1029/2000rg000101, 2002.

Waugh, D. W., Hall, T. M., and Haine, T. W. N.: Relationships among tracer ages, Journal of Geophysical Research: Oceans, 108, 3138, https://doi.org/10.1029/2002JC001325, 2003.

Wilson, R.: Turbulent diffusivity in the free atmosphere inferred from MST radar measurements: a review, Annales Gephysicae, 22, 3869–3887, https://doi.org/10.5194/angeo-22-3869-2004, 2004.

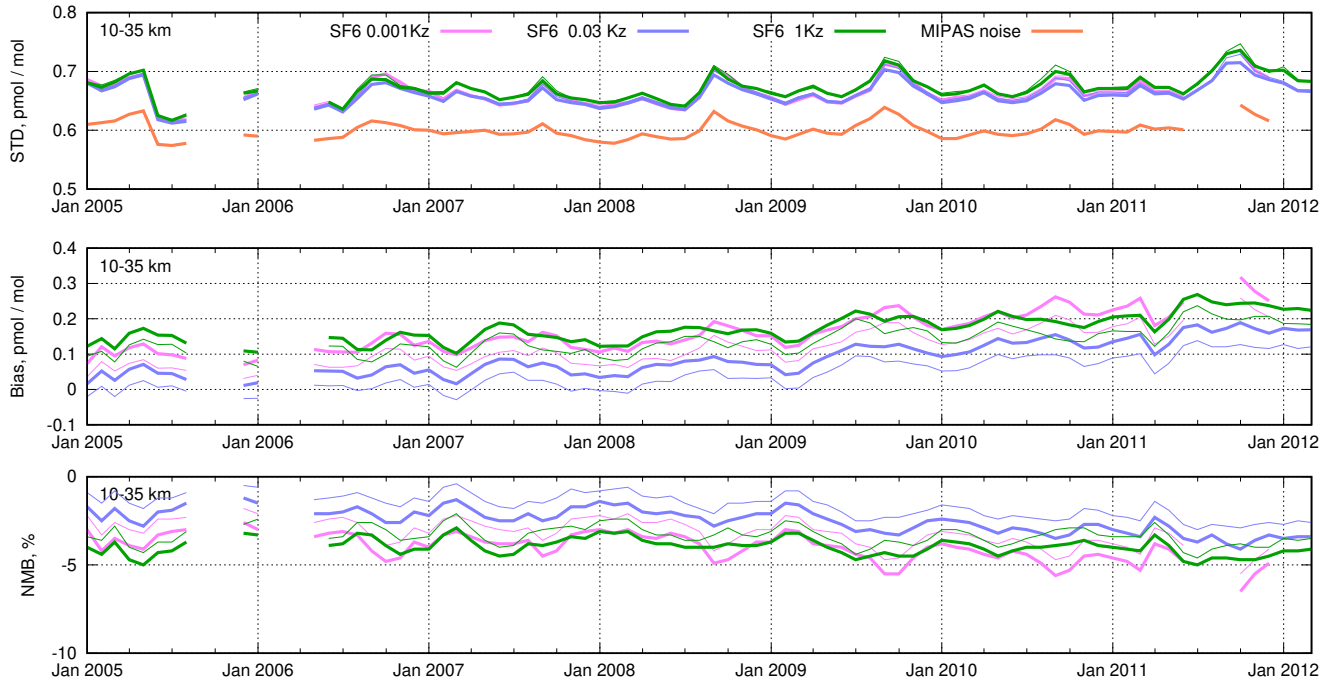

Figure 7. The time series of monthly scores for the SILAM-simulated SF_6 mixing ratios for the whole period of MIPAS observations in the altitude range of $10 - 35$ km. The statistics are ~~: de-biased RMSE~~standard deviation of model-measurement difference (STD), absolute bias and normalised mean bias (NMB). The statistics of model mixing ratios extracted at nominal MIPAS altitudes are given in thin lines.

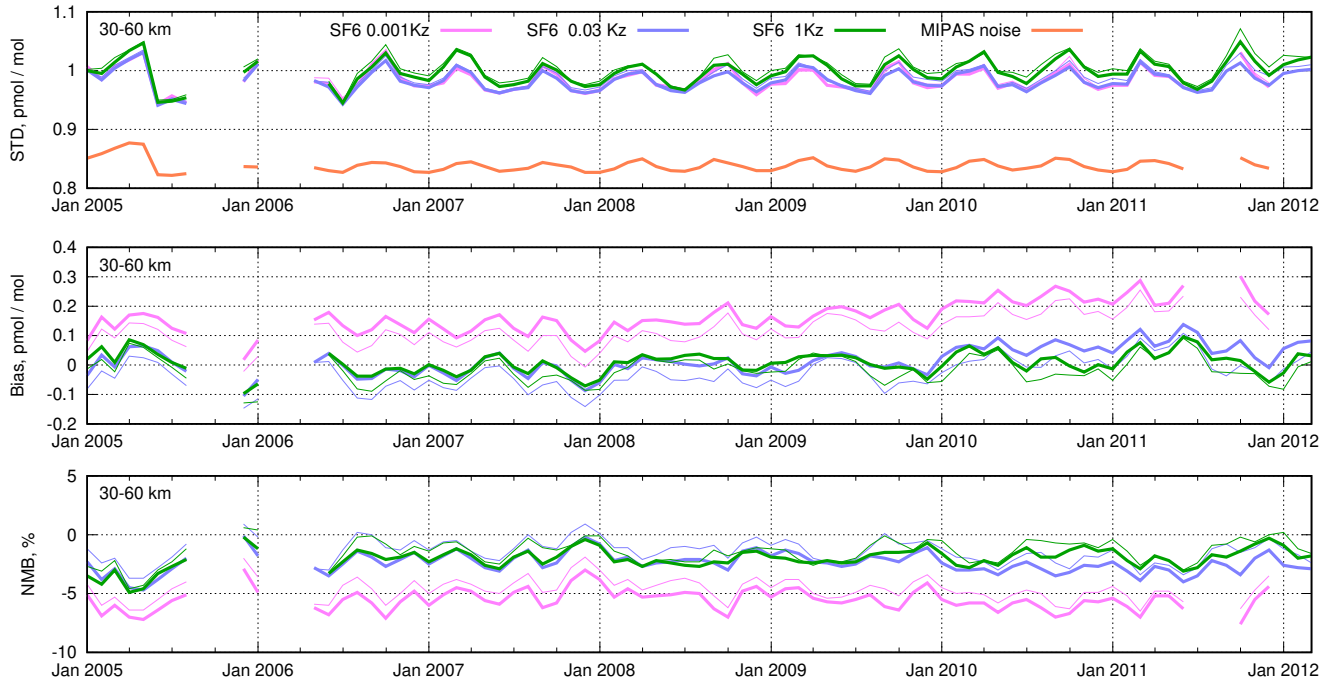

Figure 8. Same as in Fig. 7, but for the MIPAS altitude range of $30 - 60\,\mathrm{km}$.

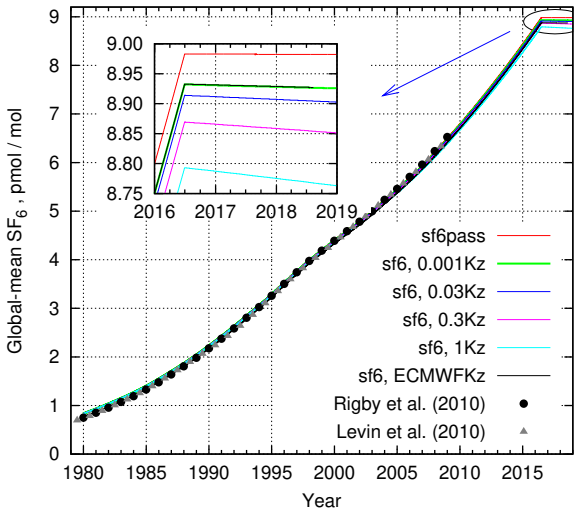

Figure 9. The time series of mean mixing ratio of SF_6 in the atmosphere simulated with emissions stopped in July 2016. The total burdens by Levin et al. (2010) and by Rigby et al. (2010) are shown for comparison.

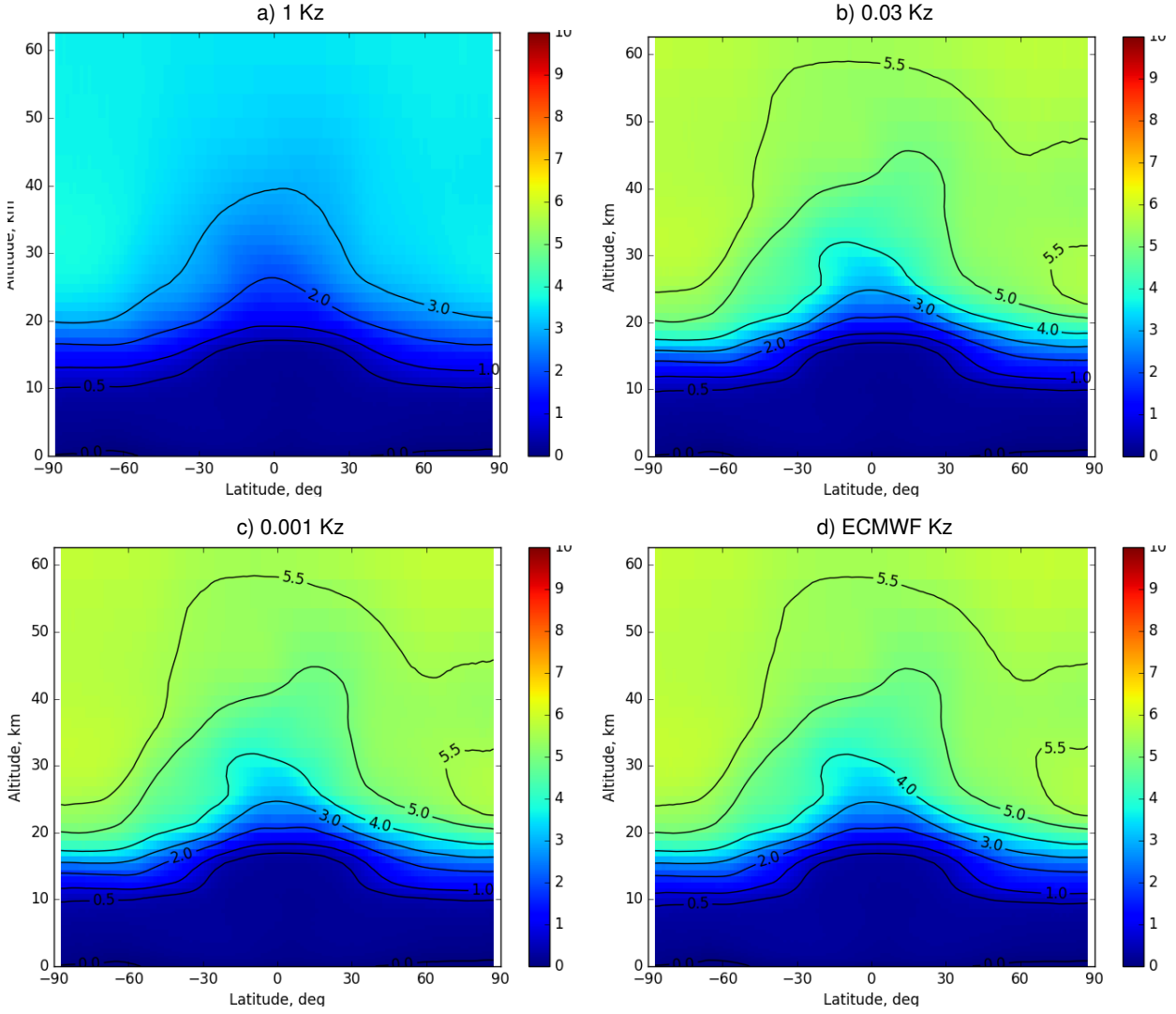

Figure 10. The zonal-mean spatial distribution of the ideal-age AoA for 2011 calculated for different eddy-diffusivity profiles.

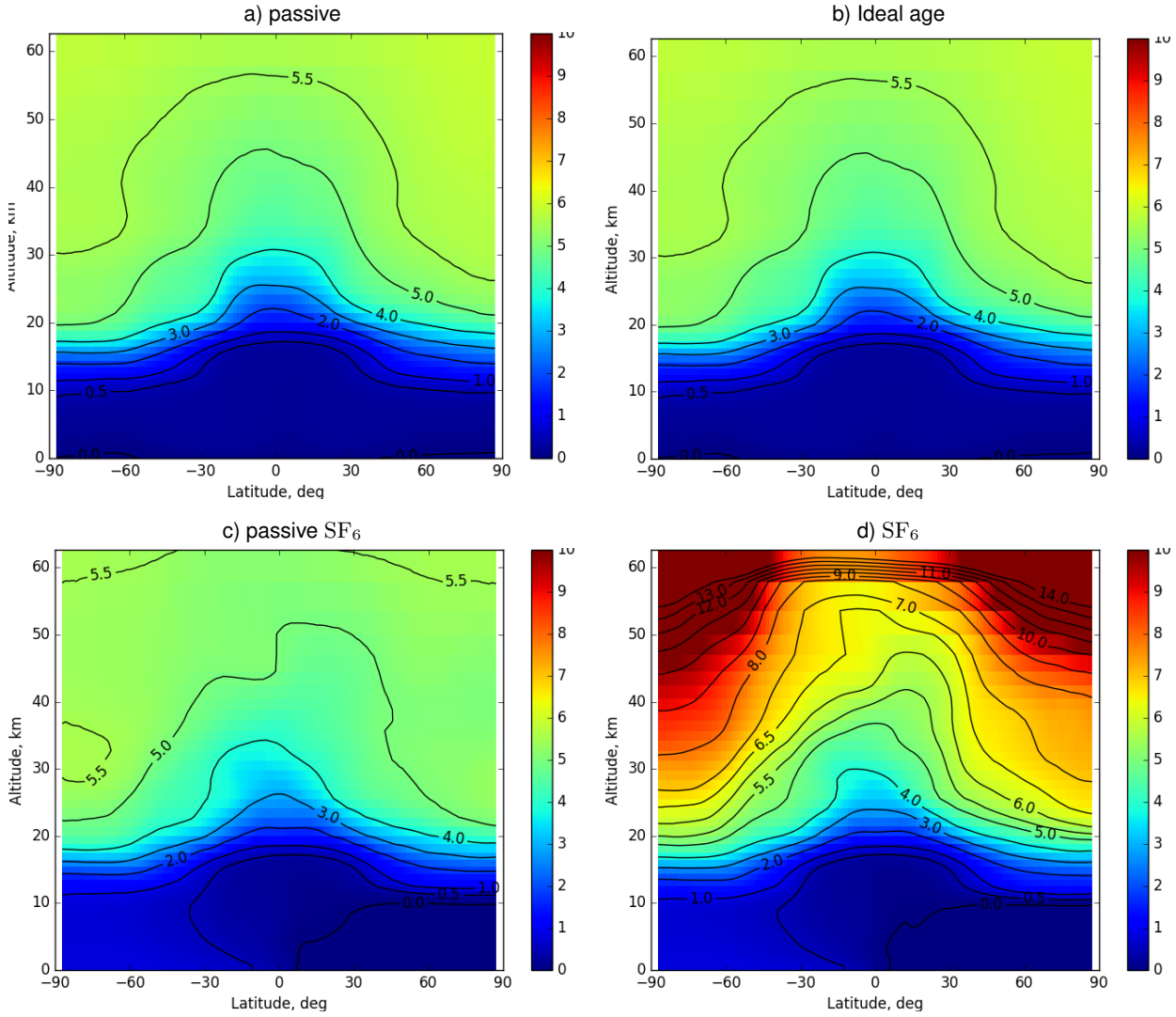

Figure 11. Zonal-mean distributions of atmospheric AoA simulated with "passive", ideal-age, and two SF_6 tracers, average for 2012.

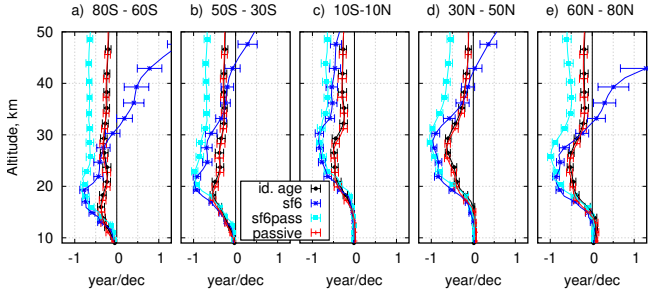

Figure 12. Vertical profiles of the simulated age of air linear trends over 11 years 2002-2012 for example latitude belts.

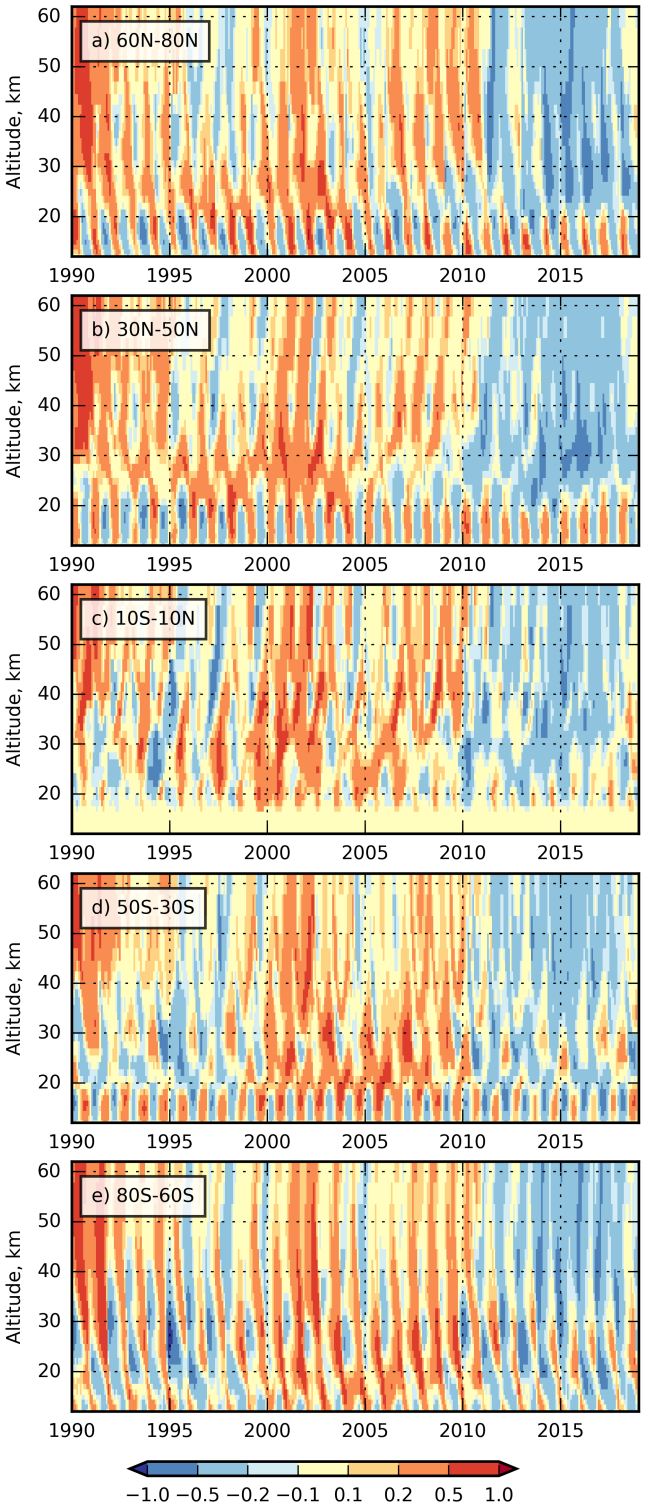

Figure 13. Anomaly of the ideal-age AoA (years) for the period of 1990-2018 with respect of the mean AoA over the same period

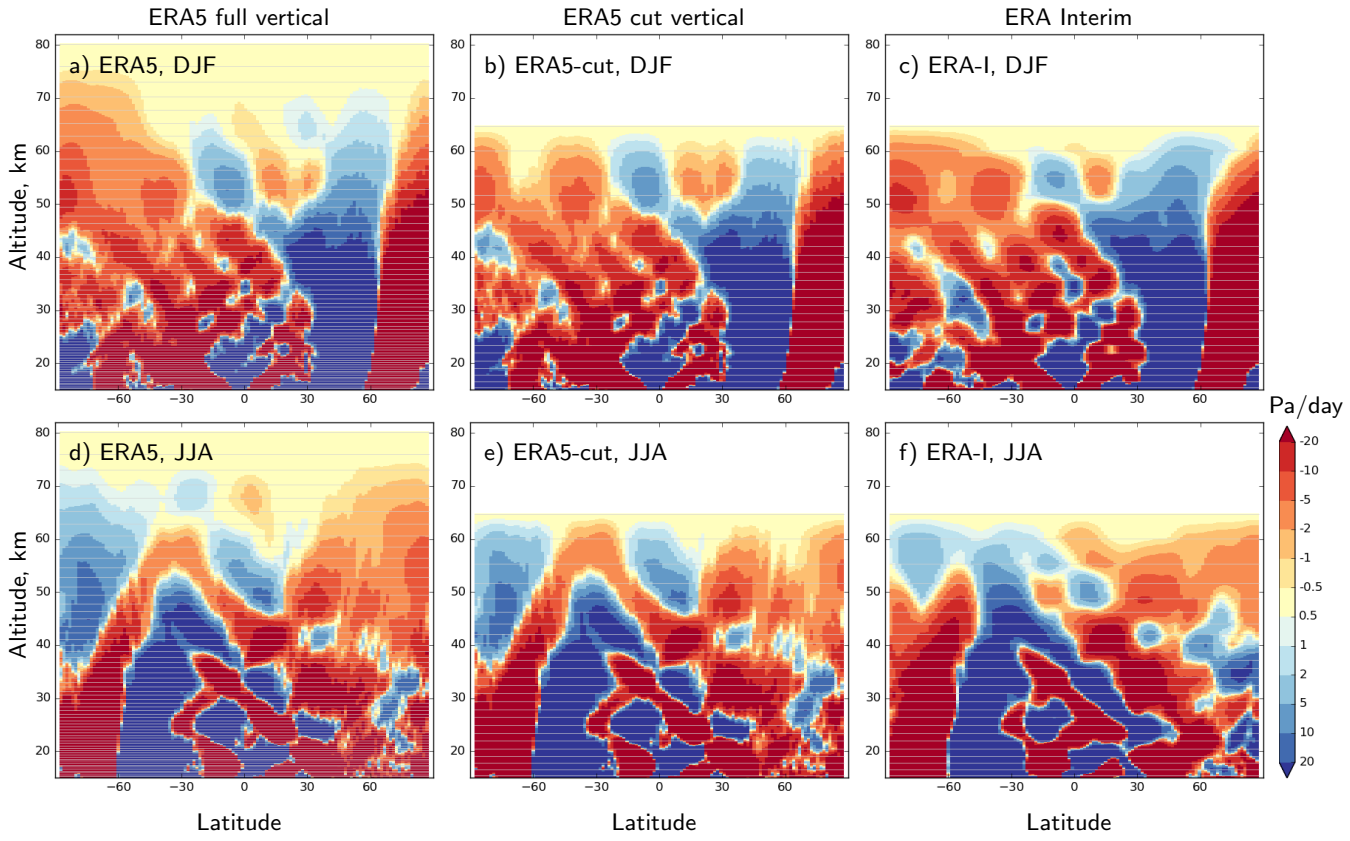

Figure 14. The seasonal and zonal-mean vertical air-mass fluxes diagnosed by SILAM from ERA5 and ERA-Interim fields for 2017 solstice seasons, expressed in terms of vertical velocity ω. Updrafts are red. The vertical-layers boundaries are shown with grey lines.